UNIVERSITÀ DEGLI STUDI DI PADOVA

DIPARTIMENTO DI BIOLOGIA

Corso di Laurea magistrale in Molecular Biology

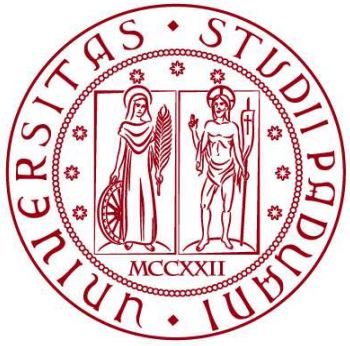

TESI DI LAUREA

Chemically fuelled deracemization of amino acids.

Relatore: Prof. Leonard Jan Prins
Dipartimento di Chimica

Correlatore: Dott. Luca Gabrielli
Dipartimento di Chimica

Laureanda: Alice Del Vecchio

ANNO ACCADEMICO 2021/2022

INDEX

1. ABSTRACT

Systems that work **out-of-equilibrium** are common in nature, living organisms are the most striking example of that.

Chemists are trying to mimic living organisms because of the multitude of properties that might be implemented in synthetic systems. With this project we want to realize an out-of-equilibrium system in which chemical fuel consumption is used to shift the equilibrium between L- and D-**amino acids**

The system presented is composed of a starting equilibrium between the enantiomers of an amino acid or a derivative. From that starting point we create an ester, mediated by a **chemical fuel** able to convert a carboxylic acid into an ester. The use of an enantiomerically pure chiral fuel would lead to the formation of diastereomeric esters and, consequently, the equilibrium would shift in favour of the more stable one under conditions where racemization of the stereocenter of the amino acid takes place.

Ester hydrolysis induced by the presence of a **chiral catalyst**, drives our system to the original amino acids but enriched in one of the enantiomers. This enantiomeric enrichment can only be maintained as long as ester formation and hydrolysis occur. In this thesis, the attention was focused on finding the best molecules and conditions to implement the system described above.

2. INTRODUCTION

The second principle of thermodynamics affirms that in an isolated physical system, **entropy** tends to increase. However, living organisms grow, move, perform functions, and increase complexity by creating order out of disorder [1]. The remarkable feature of life is that it is entropically disfavoured: a highly organized state is maintained at the expense of energy.

When we talk about chemical reactions, we refer to transformations that involve one or more reagents turning into one or more products. They can be either reversible or irreversible, depending on whether the products can return to the reagent state or not. Reversible reactions can be distinguished between those that are able to reach the equilibrium (or a nearby state) and those that are **far from equilibrium** as a consequence of external constraints.

Out-of-equilibrium systems, which are common in nature, are dissipative, implying that they require energy dissipation. This definition agrees with the description of the way they work; they consume energy to increase their order, by releasing disorder in the surrounding environment coherent with the Second Law of Thermodynamics [2].

The interest in the last type of systems arose by the multitude of new perspectives that emerge from implementing procedures leading to out-of-equilibrium conditions in a synthetic context. Reaching this aim is possible by using **chemical fuels** as source of energy. The high chemical potential of chemical fuels permits exploitation of that potential to perform transformations and functions before they are turned into waste with lower chemical potential.

2.1. CHEMICALLY FUELLED SYSTEMS

A chemically fuelled system is composed of one or more reactions that are activated in the presence of a **chemical fuel**. The chemical fuel promotes a certain chemical transformation of the systems' components and is turned into **waste**. Following a more restricted definition, the term chemical fuel is exclusively used when the system can exploit the chemical energy potential of the fuel to carry out work.

A chemical fuel that is commonly used in living organisms is **ATP** (adenosine triphosphate) whose bounds are highly energetic. The energy released from the cleavage of the terminal phosphate group allows cells to perform many different tasks that would not be possible by simply following the chemical equilibrium of the corresponding reactions. Upon reaction, ATP is turned into ADP (adenosine diphosphate) and inorganic phosphate, the corresponding waste molecules.

Chemical fuels are fundamental for synthetic systems too. With them we are able to trigger reactions that, otherwise, would not happen in a reasonable time or would not happen at all. They can, for instance, drive a system away from equilibrium.

The importance of the presence of chemical fuels in driving a system away from the equilibrium mainly resides in the fact that they have a high **chemical potential** that can be transferred to other molecules. In addition to this fundamental property, to increase their affinity towards the target compound, they can incorporate peculiar **recognition motifs** and/or structural constraints (such as stereocenters) that may affect the transfer of chemical energy from fuel to the system components.

In order to obtain a highly performing system, the coupling between fuel and system should not be limited to structural affinity between fuels and molecular machinery. It should be extended to the **kinetic** level. This means that the rate at which the energy is released should be consistent with the rate at which the fuel is transformed into waste. Since the fuel is usually chosen to be stable, the catalytic properties of the molecular machine in catalysing the transformation from fuel to waste are essential.

A chemically fuelled system is usually composed of different reactions. From a thermodynamic point of view, it should be able to cycle in both clockwise and counterclockwise directions, that are I-II*-III*-IV-I and I-IV-III*-II*-I respectively (Figure 1). However, under non-equilibrium conditions detailed balance is broken and preferred directionality takes place. A solution to this natural tendence is the implementation of **directional bias** to the cycling factor, driving the process towards anisotropy [3]. We can consider, for example, a system composed by two different equilibria (Figure 1). The interconversion between state I and state VI corresponds to the first one, meanwhile the second involves the interconversion of state II* into state III*. The passage from the first equilibrium to the second one is mediated by the preferential reaction of state I with the fuel, meanwhile the waste-forming reaction occurs faster for state III* rather than for state II*. The consequence of the kinetic asymmetry describing each reaction that interconnects the equilibria, is the creation of a directional bias to the cycling machine.

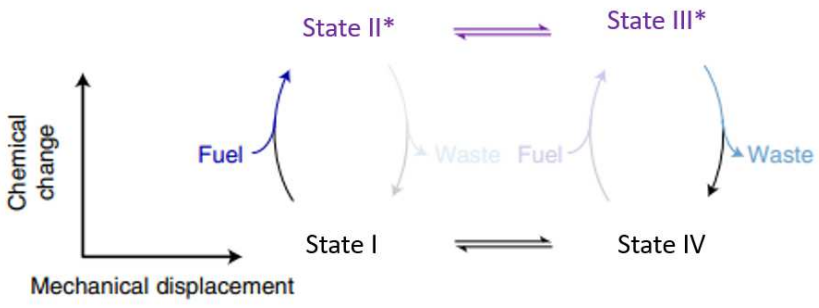

Figure 1. Scheme of a directionally biased system that is determined by different rates of fuel-mediated reaction and waste-forming reaction.

Combining all these features, we should be able to design finely tuned synthetic systems. Yet, putting in practise all requirements is more challenging than it might seem. In the following part I will describe some examples of synthetic non-equilibrium systems that have been implemented in the hard path of chemists towards mimicking the perfect life-like machine.

Relevant examples are shown in the **self-assembly** of small molecules into large structures [5,6,7,8] and **molecular machines** that exploit chemical energy are another class of important chemically fuelled systems [9,10,11].

2.2. SELF-ASSEMBLED SYSTEMS

Driven self-assembled system is defined as a dissipative self-assembly process leading to energy storage in a high-energy aggregate, as a consequence of kinetic asymmetry in energy consumption [4].

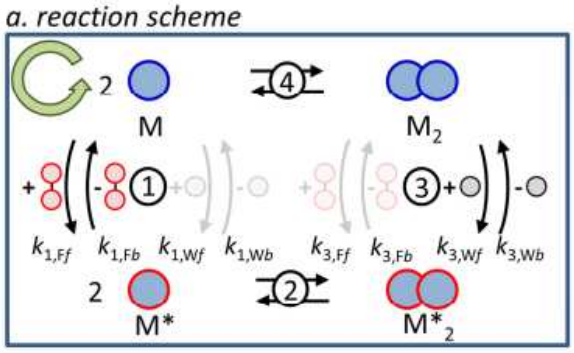

Figure 2. General scheme to represent a driven self-assembly system [5]. Chemical fuel mediated activation of the monomer (1) leads to dimers formation following the underlined equilibrium of this species (2). The transformation of fuel into waste (3) drives the monomers of the dimers to the inactive state, consequently obtaining again the free monomers in solution (4).

A typical driven self-assembled system (Figure 2) starts from the presence of the monomers in solution in the inactive form (M). Upon the interaction with the fuel, they get activated (M*) and can assemble with other building blocks to compose a more complex and functional structure (M^*_2). This state is able to stay in that configuration as soon as the fuel does not transform into waste, due to monomers or enzymatic catalysis, leading to an instable assembly (M_2) that collapses releasing all the components in the environment again (Figure 2).

Driven self-assembly not only implies the coupling between the fuel-to-waste conversion and the transformations that involve the building block, but also that the chemical energy release is used by the system to drive itself away from the equilibrium. That is, the composition between M and M_2 is different

from the composition at thermodynamic equilibrium. This requires the presence of **kinetic asymmetry** inside the wanted process [5].

The energy is not used either way by the forward and backward reaction, as it might happen taking into consideration thermodynamically driven systems, and the reactants are preferentially moved towards one rather than the other direction of cyclic systems. This **directionality** has a kinetic origin, and it depends on the fact that the rate constants of each process are finely tuned in a way that they allow just one possible grade of freedom [4].

The aim of systems designed like this is the possibility to populate a **high energy** state (M_2) that may subsequently exploit the stored potential energy to carry out tasks. In order to do so, the high energy state requires a certain kinetic stability that will assure its existence for time enough to fulfil peculiar functions. In the end, the combination between the right components – both building blocks and chemical fuels – and the right experimental conditions is the key element to accomplish all what was described before.

The first example of driven self-assembly processes that I will present comes from nature, and, in particular, it is represented by **microtubules** assembly and disassembly driven by GTP (Figure 3). These structures are present inside the cells and are involved in many processes, such as giving cellular shape, intracellular transport and chromosome segregation. The dynamic instability that characterizes them is highly useful for their functioning. It allows them to form only when they are needed, and to disassemble when there is no need of them, just on the basis of the amount of GTP present in the environment.

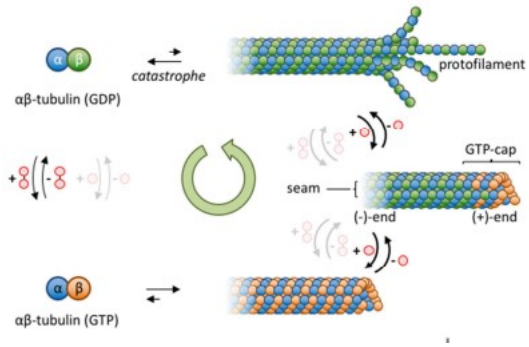

Figure 3. Microtubules cyclic formation and decomposition occurring inside cells [5]. The tubulin dimer (top-left) gets activated by GTP exchange (bottom-left) and it assembles at the plus end of the growing microtubule (bottom-right). The GTP get hydrolysed to GDP in the assembly, consequently leading to the disruption of the structure (top-right) and to the dimers free in solution again.

Alpha and beta tubulin together form a heterodimer representing the building block of microtubules. The inactive form is bound to GDP (guanosine diphosphate, the waste) and it is free in the environment. Upon the exchange of GDP for **GTP** (guanosine triphosphate, the fuel), the monomers get activated

and are able to assemble at the level of the (+)-end of the polymer, forming in the end the microtubule lattice.

In the assembly, tubulins can catalyse the conversion of GTP into GDP and inorganic phosphate. As said before, the thermodynamically most favoured state of monomers binding GDP is the free one. However, once they are packed inside the macrostructure, they are not free to disassemble, hence giving rise to the out-of-equilibrium state of the system. The conversion of the fuel into waste induces a change in the microtubule structure that increase the **lattice strain**, accumulating the energy released by GTP inside the structure.

The immediate collapse of the structure is avoided by the presence of a **GTP-cap** at the plus end of the microtubule too, that is probably given by a delay between the binding of GTP-tubulins to the assembly and GTP hydrolysis. The higher is the presence of GTP in the environment the bigger is the GTP-cap and the microtubule keeps on growing. As soon as, this cap is no more big enough to protect the (+)-end from the environment, the collapse starts, and monomers are now free again in the cytoplasm under the GDP associated form.

In that kind of system, **asymmetry** is given by the characteristics of the active site of beta tubulins (E-site). It allows the exchange of the nucleotide when the monomer is in the free state, and GTP is chemically stable. When the building block is incorporated in the microtubules, instead, the E-site changes, nucleotides are no more able to exchange and are hydrolysed. These differences in the active site between the free and bounded state of the monomer, make this whole system able to turn in one direction only, a fundamental feature for finely tuned systems [5].

Inspired by this natural example, synthetic self-assembled systems have been realized in the past years to mimic life-like behaviours. The ones implemented by Boekhoven, Van Esch et al [6,7] are good examples.

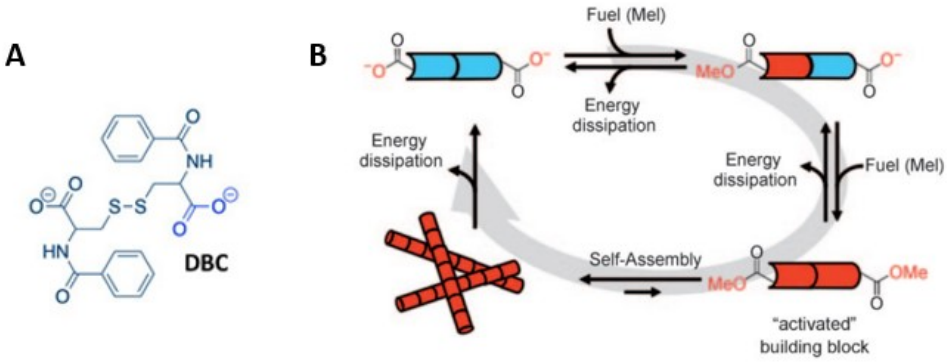

Figure 4. (A) Structure of DBC. (B) Synthetic system mimicking the biological functioning of microtubules [6]. The inactive form of DBC (Dibenzoyl-(L)-cysteine, top-left) gets activated by the action with MeI, thus obtaining the monoester (top-right). Due to the abundance of MeI in solution, also the second carboxylic site can be esterified (bottom-right). It is now able to self-assemble (bottom-left) as soon as the additional methyl group does not get hydrolysed, thus obtaining again the starting form of DBC through energy dissipation (top-left)

Under non-equilibrium conditions it is possible to obtain structures resembling microtubules starting from monomers that a chemical fuel can activate. **Dibenzoyl-(L)-cysteine** (DBC) is a known pH-responsive hydrogelator whose properties are given by the presence of two carboxylic group inside the molecule (Figure 4A).

Above their pK_a (around 4.5) these groups present a negative charge that creates intermolecular repulsion. The assembly between different building blocks is consequently forbidden as soon as the pH is not reduced below the corresponding **pK_a**. Upon the acidification, the negative charges are no more present inside the molecules allowing them to interact with each other through the formation of hydrogen bonds and hydrophobic interactions, forming elongated fibres in the end.

The authors anticipated that by chemically modifying the carboxylic group into an ester, they would have been able to trigger the self-assembly process. They realised this by **esterifying** the negatively charged group, using MeI, and, consequently, they observed that when the diester form of DBC is present in solution at high enough concentrations, fibrous aggregates formed. Because of the fuel consumption – from -COOMe to MeOH upon hydrolysis of the newly formed esters – the system is restored to the original monomeric state (Figure 4B).

The experimental conditions were optimized in order to assure a certain directionality to the system – thus implementing kinetic **asymmetry**. It represented a good starting point to later implement a new self-assembling system with better performances, as the one they have realised in 2015 [7].

In a more recent work, the research group started by using not only DBC as their switchable element, but they studied alternative building blocks (Figure 5A). These complex molecules showed one or more sites prone for esterification. The chemical activating reaction was still the esterification that is now promoted by a new fuel, the **dimethyl sulfate** (DMS) that was chosen because of its higher reactivity in respect to MeI. The chemical deactivation reaction was still represented by the ester hydrolysis induced by the presence of water, and more specifically by the abundance of -OH group inside the solution due to the basic environment (hydrolytic conditions).

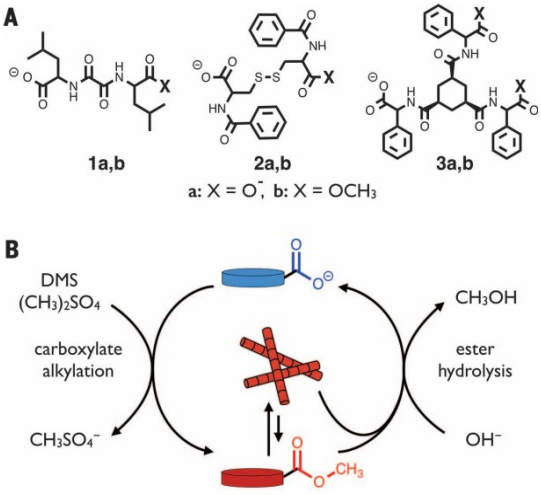

Figure 5. The second self-assembly system realized by Joe Boekhoven et al. (A) We have the structures of the switchable elements they used in performing their studies. (B) We have the general mechanism of the system implemented, as explained in figure 4 [7].

This new system (Figure 5B) was able to produce a **transient high energy state** that lasted as long as fuel was present. They were even able to verify system regeneration, that means its ability to carry out another chemically fuelled cycle after fuel-depletion.

R. V. Ulijn et al [8] presented another example of a driven self-assembly process. It differs from the others since it is activated by enzymes. In this case we have the formation of **supramolecular peptide nanofibers**. They are fibres composed by the assembly of dipeptides through π-stacking of the aromatic cycle of the molecules and hydrogen bonds. The latter occurs between peptide backbones. The starting compound is composed by a tyrosine methyl ester with a naphthoxyacetyl group at N-terminus (Nap-Y-OMe, Figure 6.1). This molecule represents the acyl donor. The proteases α-chymotrypsin, instead – apart from hydrolysing peptides – is also able to produce peptides starting from suitable ester precursors.

In this project, the protease catalyses peptide synthesis between an amide functionalized amino acid – functionalized at C-terminus – and Nap-Y-OMe, that is further favoured by the peptides' ability of assembling (Figure 6.2). Since the enzyme is a protease, the peptide hydrolysis will eventually win over the polymerization over time, consequently reaching the specific thermodynamic equilibrium. At first peptide-bond formation is faster than ester hydrolysis, leading to the assembly because of the peptide concentration exceeding the critical gelation concentration. After that, the equilibrium established between peptide hydrolysis and dimerization (between molecules 2 and 3 plus 4, mediated by both chymotrypsin and thermolysin) will be reached. If the final concentration of the dimer is higher than the CGC (critical gelation concentration), then the state away from the equilibrium was never reached. Instead, if at the thermodynamic equilibrium the CGC is not

overcome, then the gel formed in these conditions is actually a state far from the equilibrium and the system is characterized by **dynamic instability** as the microtubules in living organisms.

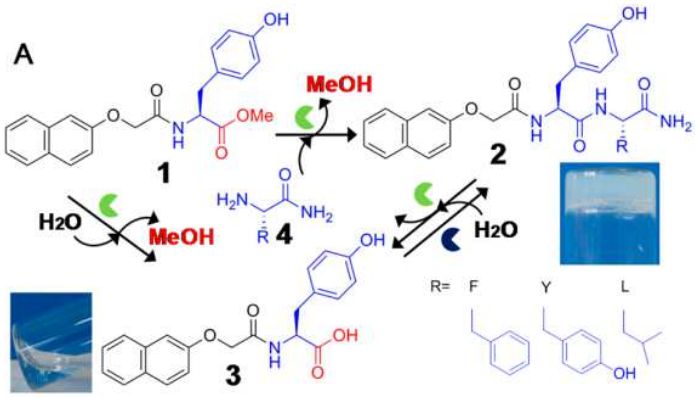

Figure 6. General scheme of enzymatic driven self-assembly system [8]. Nap-Y-OMe (1) can either be polymerized (2) or hydrolysed in the ester moiety (3) by chymotrypsin (green). The equilibrium established between these two conformations is maintained by the opposed intervention of chymotrypsin and thermolysin (blue).

The perspectives given by these three projects are striking since they clearly show that synthetic systems are effectively able to mimic living organisms' behaviour and to escape the natural tendence of simply following thermodynamic equilibrium. This opens new possibilities that are still to be explored and that can be seen even in the second category of systems driven out of equilibrium: **molecular machines**.

2.3. MOLECULAR MACHINES

In living organisms, molecular machines are represented by **molecular motor proteins** for instance. These are complex proteins able to perform autonomous movement by converting chemical energy – from a chemical fuel – into mechanical work. Among them the most notorious are myosins, dyneins and kinesins which use cytoskeletal elements as track and their movement is driven by ATP [9]. These three elements are present in nature in different forms and are essential for cells in accomplishing many fundamental tasks. They are involved in membrane transport, transport of cellular elements across the cytoplasm, adhesion of cellular components to the membrane and in many other functions. If we could imagine a living organism without myosin, dynein, and kinesin, we should think about a cytoplasm with molecules and organelles floating with no purpose inside it.

The potential energy given by the breakage of a phosphate ester in ATP is transformed by these molecular motors in **kinetic energy**. At first, we have ATP binding the active site of these molecules that, in turn, catalyse the hydrolysis of gamma phosphate group in ATP. This loss induces a conformational change of the area surrounding the active site that is then propagated in the whole molecular structure allowing it to perform a step backward or forward along the scaffold they are bound to – microtubules in the case of kinesins.

One fundamental requirement that is needed to carry out a transport function in a proper way is to follow a certain **directionality** in the movement. This can be realized by implementing specific structural features – that can involve charges interaction and repulsion for instance –, the interaction with the cargo and the interaction with the scaffold in the case of kinesin-5 Cin8 [12].

Kinesin-1 – a common kinesin inside our brain – shows two identical feet, an intertwined stalk and a tail deputed to cargo binding. The foot bound to ADP (purple in Figure 7) is found in two possible configurations that are in equilibrium at the resting state: interacting with the track or detached from it (conformer I and II respectively). The other molecular motor instead (yellow one) is unbound and strongly linked to the scaffold, at first. As soon as ATP binds the leading foot (yellow one), a conformational change occurs that together with the diffusional searching leads the detached molecular motor to a forward step. ATP hydrolysis and release of inorganic phosphate will follow to complete the cycle. Since the two molecular motors are identical, the interaction between the motor domains and the scaffold should be deputed to the directionality [13].

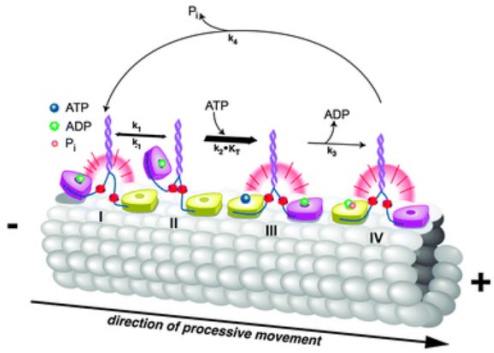

*Figure 7. Mechanochemical cycle of kinesin-1 [13]. The kinesin foot bound to ADP (violet) is free to move and it can interact with the track (I) or it can detach from it (II). As soon as ATP bind the foot strongly linked to the track (yellow), the other moves a step forward in the track (III). Then ATP gets hydrolysed, and ADP is released (IV). The synthetic counterpart of these biological motors are molecules that are able to perform autonomous **directional rotation** around a single bound, thanks to the presence of a fuel that provides the directional constraints that are needed for the movement.*

The first example of that kind of systems comes from the article of D. A. Leigh et al. [10] in which they use, as their catalysis-driven motor, the **1-phenylpyrrole 2,2'-dicarboxylic acid** (figure 8b-1a). This molecule is able to

continuously transduce the energy coming from a fuel-to-waste transformation into repetitive 360° directional rotation of the two aromatic rings composing the structure – pyrrole-2-carbonyl, the rotor, and phenyl-2-carbonil, the stator – around a N-C covalent bond.

The starting point of this cycle is the presence of the above-mentioned molecule inside a suitable solution, composed by acetonitrile and water or dioxane and water (7:3 proportion). Both the carboxylic group of the stator and the rotor are free in solution and the latter is free to rotate around the C-N bound that keeps it linked to the stator. This leads to a racemic equilibrium that is established between two limited conformations, that depends on the starting disposition of the rotor in respect to the stator – (+)-1 position, or (-)-1 position.

Due to the presence of a suitable fuel inside the solution, the two carboxylic acid groups couple to form an **anhydride**. The fuel that is used here is the N,N'-diisopropylcarbodiimmide (DIC). DIC was selected in a way to be able to react preferentially with one of the two spatial conformations composing the racemic equilibrium, introducing the first bias in the system (Figure 8a). In addition, it can react with only one carboxylic acid group present inside the molecule making it prone to the binding with the other and then transforming itself into urea (the waste). After the formation of the bounding, the hydrolysis of this bond will occur, catalysed by one of the two chiral catalysts represented in the Figure 7c. However, in order to obtain a 360° directional rotation, we must introduce in the cycle a certain **directionality restriction** and we will see how they have managed it.

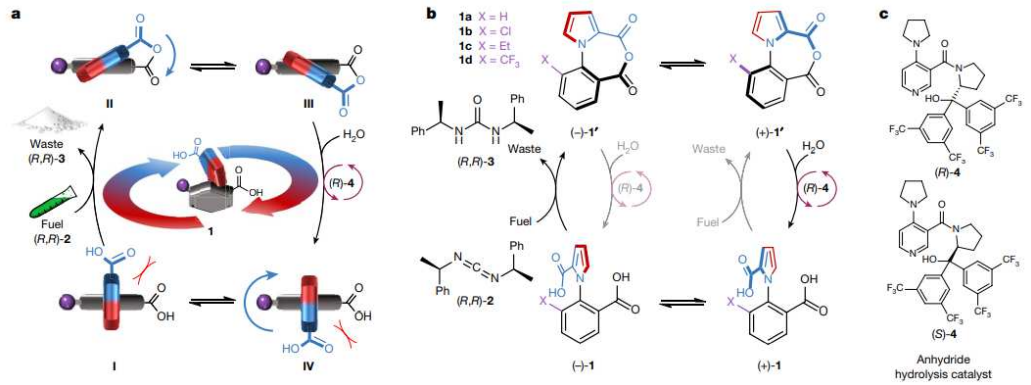

Figure 8. Molecular motor chemically fuelled [10]. (a) General scheme of the chemically fuelled rotation. We have the racemic equilibrium between starting compound (below) that is disrupted by the fuel. It leads to the equilibrium between the molecules presenting the anhydride bond (above), which is ended by catalyst mediated hydrolysis. (b) Scheme of the process they wanted to implement with insight into the structure of the molecules involved. (c) Structure of two possible anhydride hydrolysis catalyst that were used in this work.

As we have seen before, selectivity in motion can be achieved by the choice of a **chiral fuel**. A chiral compound is a molecule containing a stereocenter and

can therefore be present in two enantiomeric forms that are mirror images. The DIC derivatives used here (Figure 8b) present inside their structure two chiral centres that can be either R or S (right-handed rotation or left-handed rotation). In this project, the authors have seen that DIC in the R-R conformation was the most suitable for inducing directional rotation.

After forming the anhydride group, we have another equilibrium that is established between two opposite spatial disposition of the rotor. In this case, it would be the chiral character of the **anhydride hydrolysis catalyst** our selectivity bias that would lead to a continuum in the directionality of the system. To sum up, both chirality of the fuel and the chirality of the hydrolysis catalyst are fundamental features that allows kinetic asymmetry in the anhydride-bond forming and breaking reactions. Moreover, hiding the negative charges that are present on both carboxylic groups – by realising an anhydride bond – is fundamental, since it allows the rotation of the system around the carbon-carbon bond.

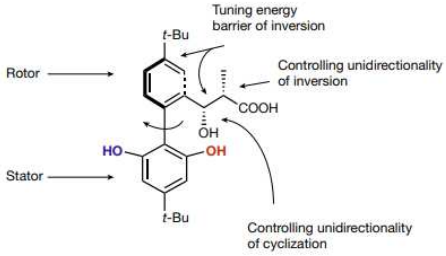

Figure 9. Structure of the molecular motor implemented by Ke Mo et al.

Compared with the molecular motor just presented, the second example of a molecular motor by Feringa et al. shows a six steps 360° directional rotation around a single C-C bound [11]. They still use the DIC as their chemical fuel in driving the formation of transient covalent bound between the rotor and the stator, however we have no more an anhydride but an ester group forming. What is more, the DIC is not the factor giving the direction bias to the system, the **rotor** now revests this role. It presents attached to the aromatic structure two different chiral centres, the first one – corresponding to the carbon in position 3 – that is in charge of the unidirectionality of cyclization, the second – corresponding to the carbon in position 2 – that drives the process of inversion towards selective direction (Figure 9).

In the first step of this system, we have the structure at the open state. Upon interaction with the fuel, the cyclization (**lactone ring**) of the molecule is promoted through an ester bond formation between the carboxylic group of the rotor and the right hydroxyl group of the stator. After that, we have the first inversion, hydrolysis induced by water and soon another lactone ring formation mediated, again, by DIC, towards the second hydroxyl group of the stator. Another inversion occurs as the previous, by establishing the position of the rotor in the most thermodynamically stable configuration and then the final hydrolysis would lead us to the system initial step. Another turn into the cycle can be promoted by the presence of further DIC (Figure 10).

Both molecular motors presented demonstrated the utility of chirality in introducing directional bias inside a system. The selectivity of the reaction increases, thus leading to transient enrichment of the solution in a certain configuration of the motor out of two possible enantiomers. This procedure of

mixture enrichment of one out of the other molecular configuration is well known in organic chemistry and is called **dynamic kinetic resolution**.

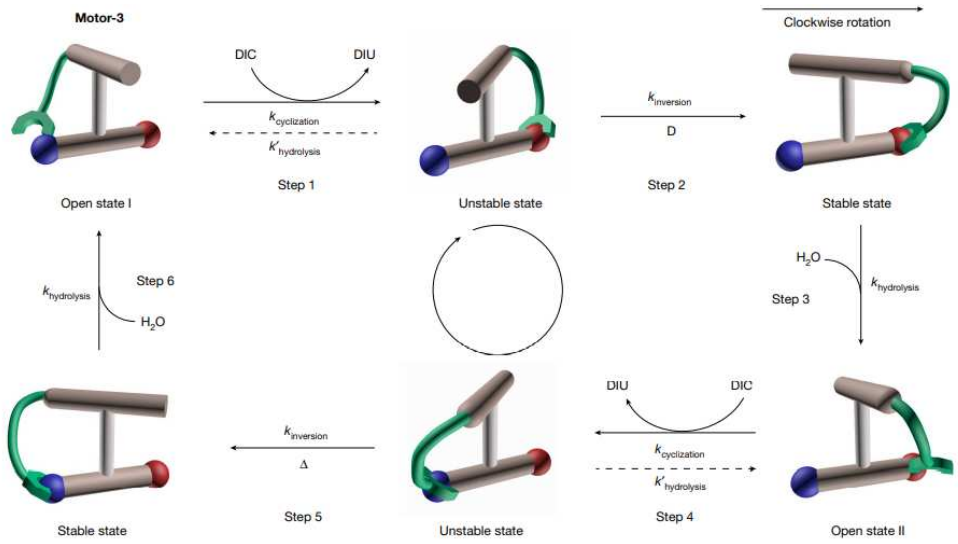

Figure 10. Schematic representation of the 6 steps directional cycle implemented by Ke Mo et al. The open state I turns into the unstable cyclized one by the action of DIC (step 1). The inversion (step 2) drives the molecule to the most stable state of this conformation that is then transformed into the second open state by water hydrolysis (step 3). Another cyclization step mediated by DIC (step 4) leads to a further inversion (step 5) of the structure. The cycle turns back to the starting point after hydrolysis (step 6).

2.4. DYNAMIC KINETIC RESOLUTION

In chemistry, **kinetic resolution** refers to the ability to separate the two enantiomers (D and L) – originating from a single chiral centre – of a racemic mixture by means of chemical reactions. The different rate of reactions of the enantiomers allows obtainment of an enantiomerically enriched solution. Starting from a racemic solution, the easiest way to accomplish this is to use enzymes. They will react with both enantiomers but at different rates, thus enriching the faster-reacting molecule configuration. These processes are defined as **deracemization** ones.

However, following the method mentioned before, we would not be able to obtain a fully enantiopure solution. In order to reach this goal, it is necessary to combine the enantioselective resolution with the racemization of the slower reacting enantiomer. In this case, the yield should be ideally 100% and the procedure is called **dynamic kinetic resolution** (DKR) [14].

Some requirements should be followed to obtain all the possible advantages in performing DKR. First, the **resolution step** should be highly selective; it means that the difference in the reactivity with the catalyst between the

wanted and unwanted reagent should be very high. In that way the undesired molecule would stay mostly non reacted in solution, instead, our target would be found mostly transformed in the desired product (Figure 11).

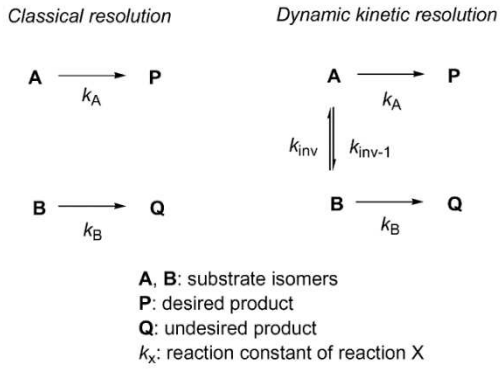

Figure 11. On the left we can find the scheme of kinetic resolution reactions. On the right we have the scheme of DKR reactions, in which Kinv should be faster than Kinv-1 [16].

A second important requirement is the **irreversibility** of the resolution step that would trap the wanted compound in the product with no chance of having the reagent back. The last one, instead, concern the difference in racemization and resolution step **rates**; the first process should occur faster that the second. The advantage is related to the possibility of having a less selective transformation, since the undesired molecule is transformed in the desired one with higher probability in respect to be subject of the catalysed process (Figure 11).

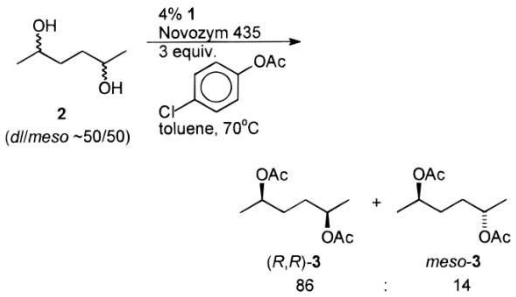

Figure 12. General scheme of the DKR performed on a racemic mixture of 2,5-hexanediol. (1) is the ruthenium catalyst [14].

One example of dynamic kinetic resolution performed in presence of an enzyme catalyst is the system that is intended to transform a racemic solution of secondary diols in an enantiomerically pure solution of (R,R)-diacetate. We have here the presence of a **ruthenium catalyst** that can favour the

isomerization of the starting diol – racemization step. In addition, we have an enzyme to catalyse the acylation reaction that occurs in the presence of an acyl donor (Figure 12).

The reaction was improved by using different experimental conditions and changing the acyl donor structure. It was observed that modifying the second parameter by increasing the dimension of this element, a higher **diastereoselectivity** was accomplished. As a consequence, we have in that way increased the rate of the desired molecule transformation [15].

Dynamic kinetic resolution is performed too on alpha amino acid esters in the presence of **aldehydes**. In this case, the resolution step is performed by using a lipase catalysing ester hydrolysis, instead the racemization was induced using salicylaldehyde for instance (Figure 13).

Aldehydes in solution form imine with the alpha-amino acid ester N-terminus. The imine is particularly stable because of hydrogen bond realized between the imine nitrogen and the hydroxyl group of salicylaldehyde (**Schiff base**). The racemization of the alpha carbon is highly favoured in this way because of the increase in the stability of the carbanion forming as a racemization intermediate. The negative charge is delocalized on the aromatic system conjugated to the imine bond. The additional presence of electron-withdrawing groups (such as nitro groups) will behave like further stabilizer of the negative charge by attracting electrons [16].

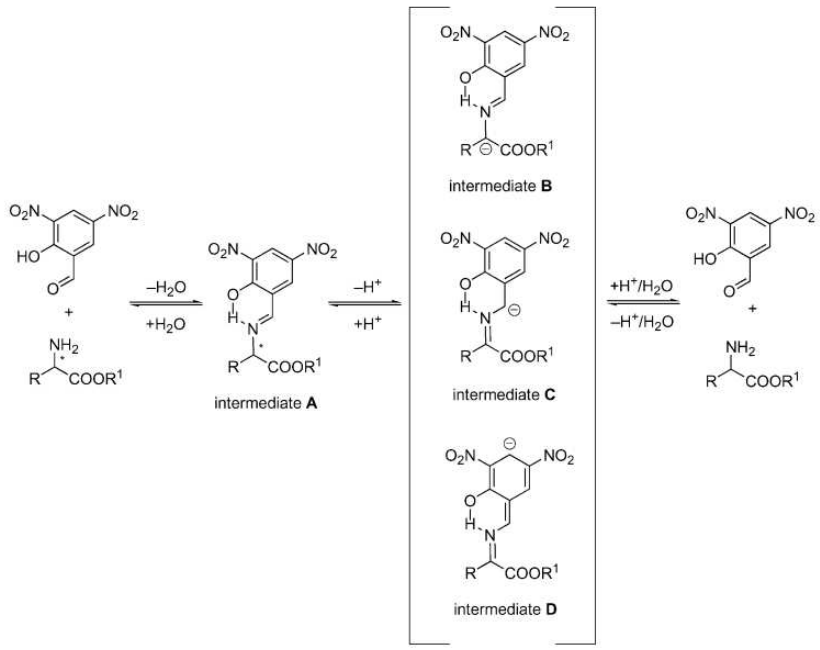

Figure 13. Possible mechanism for aldehyde-catalysed racemization of alpha-amino acids (here 3,5-dinitrosalicylaldehyde). The reaction between the aldehyde and the compound leads to the formation of the corresponding Schiff base. In this conformation the acidity of the carbon in alpha position is high enough and it is able to lose its hydrogen. The hydrolysis of the complex releases the racemized amino acid and the aldehyde.

These two examples of DKR used a different approach to increase the rate of the racemization step, however they pursued in the necessity of enzyme presence for the resolution one. Both molecular motors analysed in the previous section made use of dynamic kinetic resolution in order to move the system away from the equilibrium, however they used a chiral catalyst [10] or water only [11] for the resolution step. The reaction between the chemical fuel and the reactant was used with the objective of providing the molecules with the right additional group or configuration that would trigger the enantio-enrichment. In addition, DKR systems are one way only, they are irreversible, instead real-life ones – and the molecular motors presented before – are transient and reversible.

From all the assumptions and the examples described before, the aim of this project arises.

2.5. THE AIM OF THE PROJECT

I would like to start the description of the project from some well-established statements. First of all, the molecule that will be used is an amino acid or an amino acid derivative and – as we all know – every amino acid, except glycine, presents a **chiral centre** in correspondence with the alpha carbon. It means that we can have two different configurations for the same molecular object, called enantiomers (figure 14). They can be D or L depending on the spatial disposition of atoms around the chiral centre.

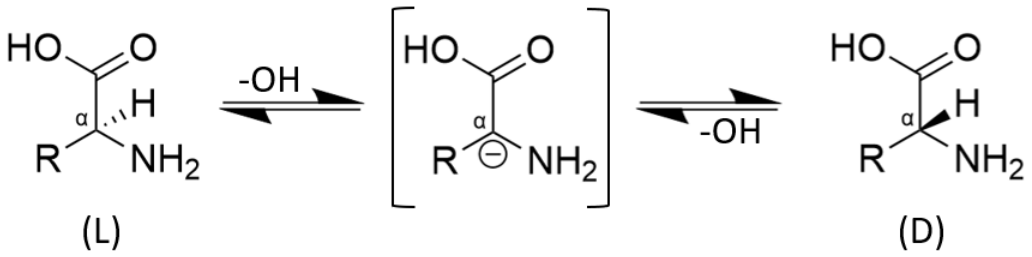

Figure 14. General equilibrium existing between two conformations of the same molecule (amino acids here).

In living organisms, we can observe the presence of **L enantiomers** only, the reason why nature adopted this building remain without a reasonable explanation. There is no evident reason for which one conformation should have been chosen instead of the other, that is why during production processes of amino acids we must use enzymes, kinetic resolution, or dynamic kinetic resolution procedures to obtain in the end the most enantiopure product as possible. This is of great importance in the pharmacology field mainly since

different enantiomers might interact differently or not at all with the target element.

We want to investigate whether it is possible to use chemical energy to shift the composition of a racemic mixture of **amino acids** away from thermodynamic equilibrium (50% L – 50% D) and maintain the system in a non-equilibrium state as a result of energy consumption. It means that we would still include kinetic asymmetry characteristics, chemical fuel usage, catalysts, DKR principles, out of equilibrium states, as seen before, but applying them on as simple elements as amino acids.

Our system (Figure 15) is composed of four reactions forming a cycle. The starting point is the racemic equilibrium between the two possible enantiomers of our amino acid (Figure 15A).

The chiral centre taken into consideration is the carbon in **alpha** position. It is connected to the amine group, carboxylic acid, lateral chain and one hydrogen. The spatial disposition of the four substituents defines the absolute configuration of the stereo centre, defining L and D enantiomers which are present in equal quantities in the racemate.

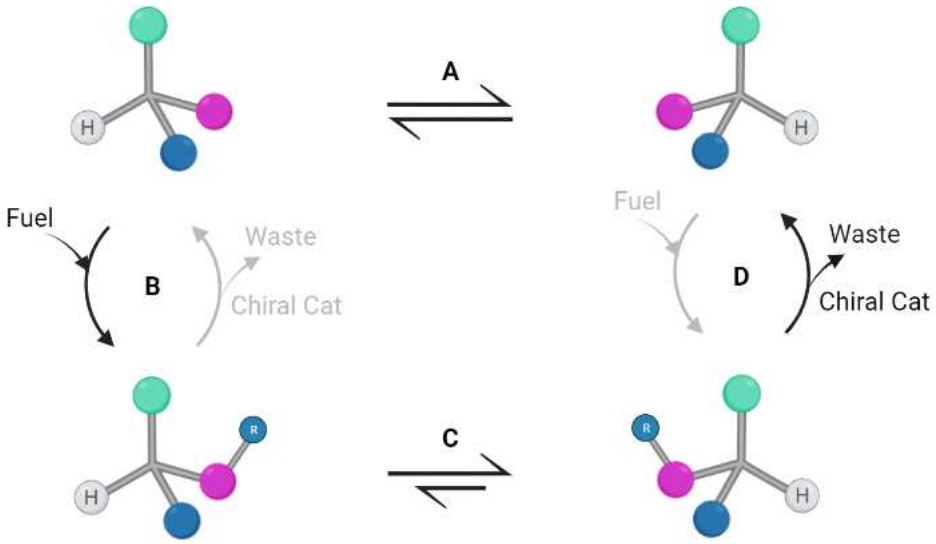

Figure 15. General scheme of the cyclic system we would like to realize. In green we have the lateral chain of the amino acids, in blue the group containing N (amine termination) and in violet the carboxylic group. The little circle containing an R indicates the chiral group that would give the enantiomeric selectivity.

At the thermodynamic equilibrium, the amino acid will be present as a racemic mixture. Indeed, the alpha proton might be acid enough to **exchange** with the protons in the solution, but because of microscopic reversibility this doesn't affect the composition of the mixture.

The molecule is activated for racemization by forming an ester bond at the carboxylic moiety using a chemical fuel [21]. Ester formation could be achieved through the addition of a carbodiimide as activating agent and an alcohol. Using this kind of fuel, we would create the first bias in the system (Figure 15B). In fact, if the **carbodiimide** is chiral, we can favour the activation of only one of the enantiomers. In this manner, once the fuel is depleted, we would have an excess of the remaining less-reactive enantiomer. Another manner to form the ester is by using a **chiral alkyl iodide**. Thus, the esters formed from the enantiomeric amino acids would be diastereoisomers. Consequently, under conditions at which racemization of these esters would take place, the equilibrium would not be 50-50 (Figure 15C).

The second kinetic bias can be inserted during the **hydrolysis** of the ester (Figure 15D). In this case, we can use a chiral catalyst that selectively hydrolyses the ester of one of the stereoisomers. In a manner analogue to the previous, if only one of the two enantiomers will be cleaved this will lead to an enantiomeric enrichment of the product. At the end, after a chemically fuelled cycle of ester-formation followed by ester hydrolysis, we would have the presence of only one of the two enantiomers of the original racemic mixture. But as said above, since spontaneous racemisation takes place under the experimental conditions, this equilibrium will be spontaneously shift back to the racemic mixture when fuel has been depleted.

The final aim of this project is the realization of a molecular **information ratchet** [5,17,19,20]. The word ratchet means that we can now realize a chemical process that presents a directional bias.

Exploring the system from an **energetic** point of view, we can see that for the first equilibrium involving the amino acids, both enantiomers have by definition the same energy level and are consequently present at equimolar concentration (Figure 16A). After the esterification, instead, changes occur in the energy diagram of the system, thus obtaining an energy difference between the species in the solution (Figure 16B). Upon equilibration this will lead to a population of the species with the most stable configuration (Figure 16C).

A further stratagem that would be applied inside this project to enrich even more the enantiopurity of the solution – and consequently reinforce the asymmetry – is the usage of kinetic resolution technique in the form of a **chiral hydrolysis catalyst**. From C to D (Figure 16), we will promote the hydrolysis of the chiral group that has been added previously from the interaction between the fuel and the initial compound, consequently releasing the waste. The use of the peculiar catalyst mentioned before, would provide a certain stereospecificity of the reaction toward one rather than the other enantiomer (Figure 16D).

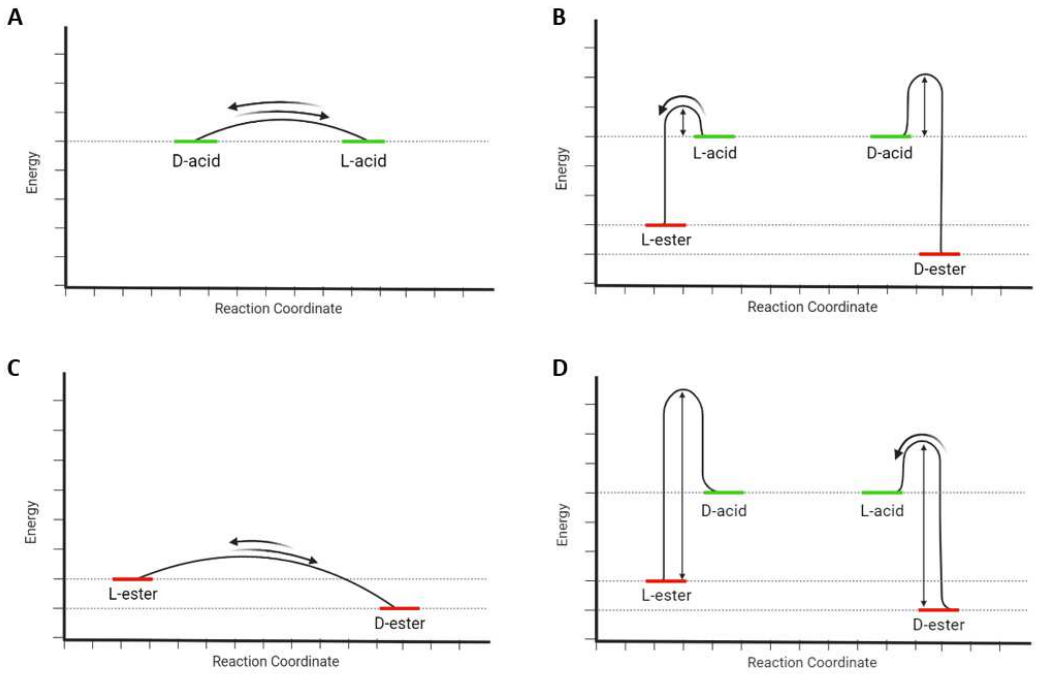

Figure 16. (A) Energetic description of the equilibrium between acid forms. (B) Energetic description of the reaction with a fuel. (C) Energetic description of equilibrium between esters. (D) Energetic description of the hydrolysis step.

Under the kinetic point of view, we need to introduce differences in the reaction rates of the two enantiomers in both the activation and hydrolysis steps. The D enantiomer in this case might show a bigger rate constant than L enantiomer being hydrolysed, consequently giving rise to an almost pure enantiomeric solution. We need to take in mind that both conformational population (ester equilibrium) and product composition (state right after hydrolysis) are interconnected, however it does not exist a direct correlation between them. The principle underling this fact is **the Curtin-Hammett** [17,18], which affirms that even though we might have an interconversion equilibrium pending more to one rather than the other conformation, the products ratio might be different than what we expect. The height of the energy barrier existing between reagent and product should be taken into consideration as well (here the ester form and the acid form respectively). However, since the hydrolysis catalyst should be designed to be highly enantioselective, we still confirm the enrichment already present in state C.

The enantiomers equilibrium moved mostly towards one configuration with the selectivity of the hydrolysis step, will give rise to a real **dynamic kinetic resolution** procedure. The state right after hydrolysis of our system is the kinetic state, in which even if the amino acid would not have a preferential distribution among the different spatial conformations, we indeed have an enrichment of D enantiomers due to the effect produced by the previous passages. Thus, in this state the system is defined out-of-equilibrium. However, since the rate constants describing the interconversion of one

enantiomer into the other – at this molecular state – are the same, we will obtain the establishment of the starting racemic equilibrium again.

In this ingenious way we are theoretically able to move the system **away from the equilibrium** in the form of an enantioenriched solution that is not thermodynamically favoured, thanks to the presence of a fuel-to-waste conversion catalysed by the cycling factor itself. Starting from these assumptions I will explain what was done in practice in order the realize this cycling system.

3. DISCUSSION and RESULTS

In order to construct the reaction cycle presented (Figure 17), we need to start by studying step-by-step **every single reaction** it is composed of. Indeed, it is important to know the kinetics of each reaction involved. Crucially, it implies that the rate of racemization of the ester must be faster that the racemization rate of the acid. In addition, the kinetics of esterification must be faster than the kinetics of ester hydrolysis.

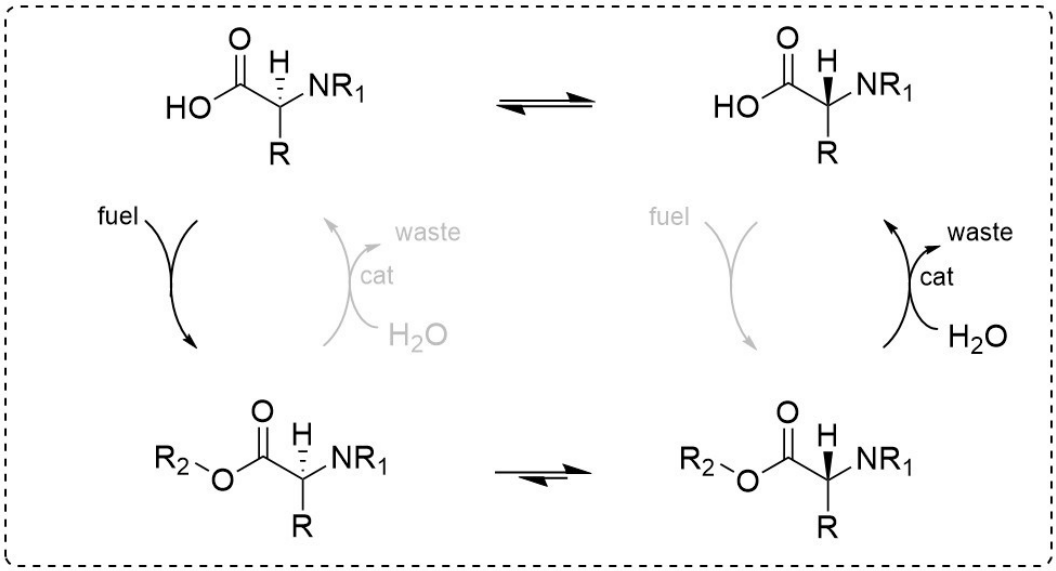

Figure 17. General scheme of our system with general structure of molecules (above). We have at first the racemic equilibrium between acid forms (top-left), then equilibrium between ester forms (bottom-left and right) and finally the hydrolysis pushing the system way from the equilibrium (top-right).

3.1. RACEMIZATION STUDIES

We started by studying the **racemization** rate of suitable compounds.

To perform racemization studies, **nuclear magnetic resonance** (NMR) was used. The NMR is an instrument recording signals coming from specific nuclei, in particular form hydrogen, carbon and fluor. For our purpose, we are interested in the signal from **hydrogens** of the target molecules. Deuterated solvents are typically used to avoid that the ^1H NMR spectrum is dominated by signals coming from solvent nuclei.

The equilibrium under investigation involves the alpha carbon, which is our chiral centre. Since we used D_2O as solvent (or cosolvent) in our studies, we would like to verify the possibility of having a **hydrogen-deuterium exchange** in solution between the hydrogen linked to the carbon in the alpha

position of our amino acid and the deuterium atoms that are present in the solution. Since deuterium nucleus is not visible with NMR, if the exchange is allowed in the experimental conditions, we would see the reduction in intensity of the alpha hydrogen signal. Importantly, H-D exchange on the C_α-carbon is an indicator for racemization. This is because the mechanism with which our molecules exchange the proton on C_α passes through the formation of a carbanion intermediate (stabilized by solvent). This intermediate has a planar configuration where the carbon assumes a sp^2 hybridization and the chirality is lost. Because the environment presents a higher concentration of deuterium compared to hydrogen it is very likely that reattachment involves a deuterium rather than hydrogen. It is important to notice that the re-attachment on the planar intermediate can occur from either top or bottom of the plane, implying that both enantiomers can form with equal probability.

We cannot use any kind of molecule to obtain an efficient hydrogen-deuterium exchange. They should be selected following specific criteria. In particular, they need to have a high grade of **alpha hydrogen acidity**. It means that the alpha carbon should be able to dissociate the hydrogen easily under the experimental conditions. Despite the C-H bond is known to be very stable, it's acidity can be tuned by the presence of electron withdrawing groups [22].

One crucial feature of our molecules is the structure of the **lateral chain**. In nature, the amino acids reported having a faster racemization are phenylalanine, histidine, and aspartic acid. Histidine possesses an imidazole as lateral chain that, because of its basic nature, can favour the extraction of proton in alpha position. Aspartic acid can make an intramolecular anhydride between the lateral and terminal carboxylic acid under certain conditions that, due to the elimination of a negative charge leads to the racemization of this molecule. In all our studies we employed only the phenyl group or benzyl group. This is because the presence of the aromatic ring in the phenyl group can favour the delocalization of the negative charge formed in the intermediate. This leads to reduction in the pK_a of alpha carbon of phenylglycine (pK_a = 19) ten orders of magnitude compared to glycine (pK_a = 29).

Figure 18. Resonance limit structures of the nitrogen together with the BOC protective group.

In addition, since the **amine group** is a good nucleophile and can therefore give side reactions during the esterification of carboxylic acid, we decided to mask it. The easiest way to do that is using a protecting group that is stable under basic conditions such as *tert*-butylcarbamate (BOC, Figure 18). Anyway,

we explored also other alternatives in order to transform the amine bond in a strong electron withdrawing group able to acidify further the proton of C-alfa.

Finally, it was chosen to activate the amino acid for racemization by forming an **ester** bond with the chemical fuel. The formation of an ester between the carboxylic acid residue and alcohol will mask the negative charge, thus increasing the acidity of hydrogen on the alpha carbon. The presence of a negative charge in the acid-form of the amino acid reduces the possibility of forming the carbanion. As shown by studies performed by Richard et al. an ester has a pKa that is 8 orders of magnitude lower than that of the free acid [24]. Indeed, an ester compared to the other protecting group such as thioester, amide and oxazoline is easier to make and it has a very well know kinetic of hydrolysis under basic conditions.

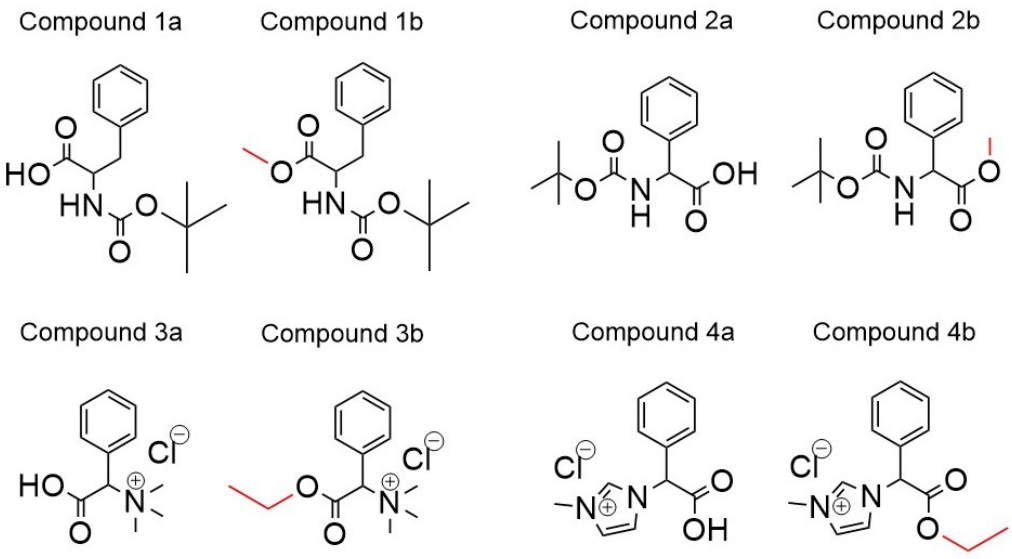

Figure 19. Specific structure of compounds used in both acid (a) and ester (b) form. The ester form presents in red the additional portion that was added by esterification.

Amino acid characteristics are not enough to obtain racemization, we must use specific experimental conditions, such as the implementation of a **basic environment** [23]. The abundance of negatively charges hydroxyde ions in solution facilitates the detachment of the hydrogen from the carbon.

Considering all these factors for the design of our molecules, we have tested four different structures (Figure 19) with increasing acidity of the alpha hydrogen. For both structures both the acidic and ester form are shown.

3.2. RACEMIZATION STUDIES: COMPOUND 1

Compound **1**, Boc-phenylalanine, is the first molecule that we used for our racemization studies (Figure 19). Its lateral chain is represented by benzyl group, instead the amino terminus of this molecule is protected by a Boc-group.

We tested three different conditions with the aim of promoting the racemization of the ester form, that was expected to be easier than the acidic one for the reasons explained before. The first two conditions were realized by placing the compound (0.01 M) in a solution composed by 7 parts of acetonitrile (ACN_{d3}) and 3 parts of deuterium oxide (D_2O) in addition to **lithium hydroxide** in different concentration to obtain e final pH value of 8 and 11. Despite the strong basic conditions of the latter, we observed no changes in the alpha hydrogen signal in both samples, thus no exchange with deuterium present in the solution even after one week recording or after placing them at 50°C. The higher temperature should have increased the reactivity of all the components, but nothing changed.

The third attempt was realized in a solution made up by 5 parts of deuterated dimethyl sulfoxide (**DMSO-d6**) and one part of deuterated methanol (**CD_3OD**). The base that was used here is **1,8-Diazabicyclo [5.4.0]undec-7-ene** (DBU) and the solution was kept at 31°C [25]. In these conditions we were able to see two processes occurring inside the sample. The first is the reduction of the peak of the hydrogen on C-alfa (Figure 20A), indicating exchange with deuterium (see Figure 20B) and this process occurs quite slowly. The second process is the exchange between the methyl ester group in the molecule and deuterated methanol present in the solution (Figure 20C, 20D) with a faster kinetic compared to racemization.

In conclusion, even if we were able to see some racemization, it is too slow, and consequently we expect that the racemization of the acid form would have been even slower. In addition, since **DMSO** is well known to catalyse the hydration of carbodiimide which is the potential fuel we to be used in our system [26], we have excluded the compound **1a** from further studies. We moved on by implementing racemization studies on a molecule with more acidic protons.

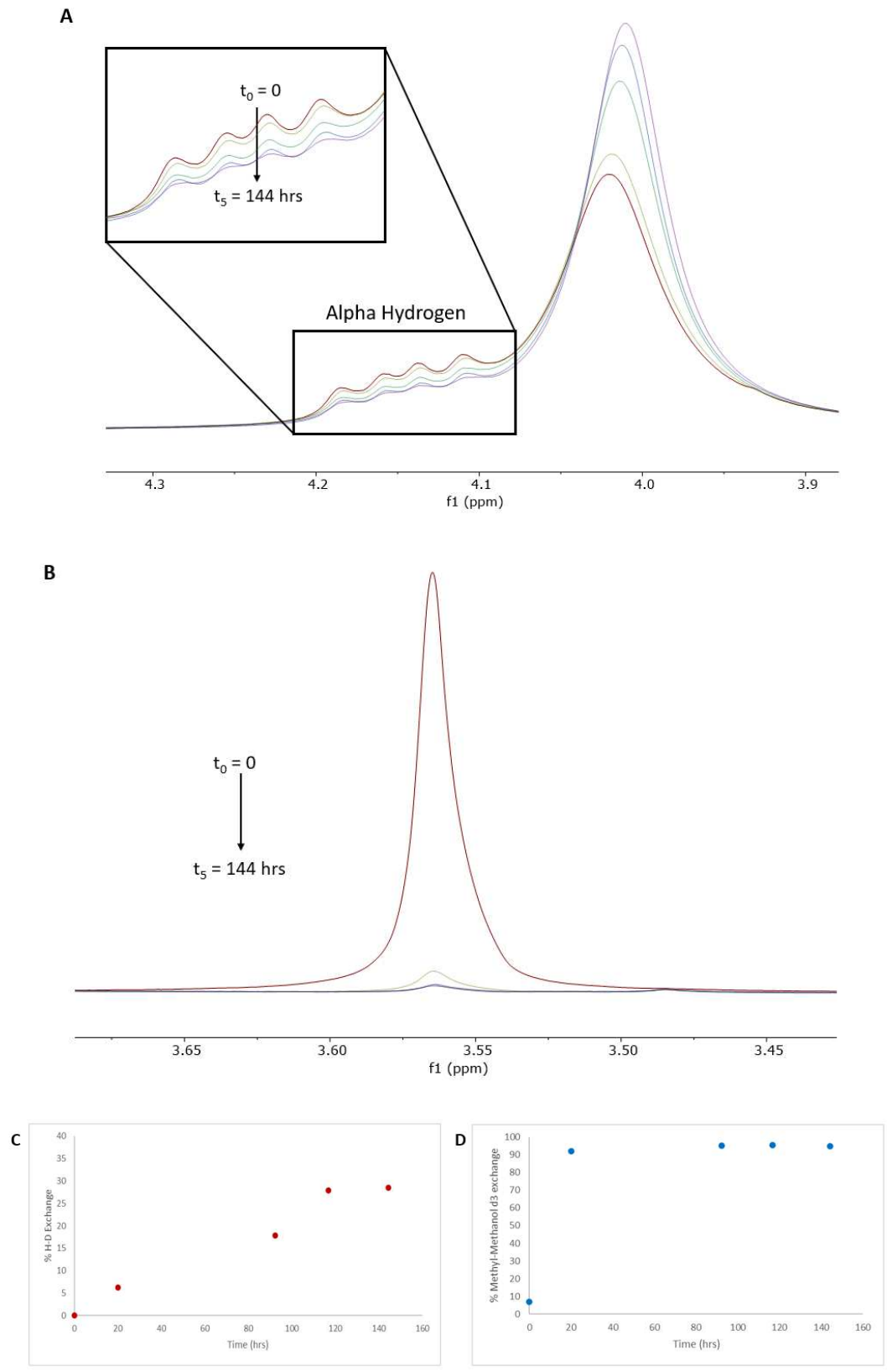

Figure 20. (A) Superimposition of spectra recorded of the sample containing phenylalanine, DBU, DMSO and methanol. The alpha hydrogen signal is the quartet on the left and it composes a full peak together with the hydrogen from the hydroxyl group of MeOH. (B) Superimposition of spectra showing the reduction of -CH_3 peak. (C) H-D exchange kinetic. (D) Kinetic of exchange between methyl group and methanol.

3.3. RACEMIZATION STUDIES: COMPOUND 2

The main difference between compounds **1** and **2** resides in the absence of the methylene-group. The removal of the methylene group – that separates the alpha carbon from the aromatic cycle in compound **1** – is expected to facilitate racemization as it permits delocalization of the intermediate negative charge. As a result, other than the small π-system of the carbonyl-group, the negative charge can delocalize on the **aromatic cycle** (Figure 21). The advantage of this structural improvement is the enhancement in the carbanion stability, hence the promotion of hydrogen-deuterium exchange, and the decrease in the associated pK_a.

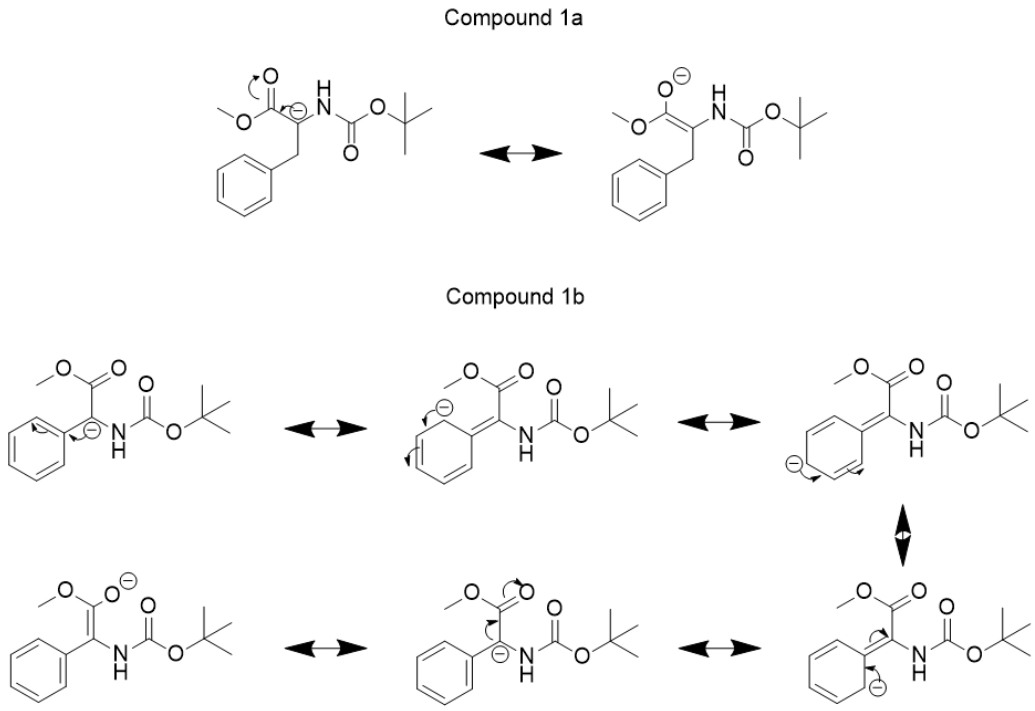

*Figure 21. Above in this image we have the resonance structure that might be given by compound 1a. Below we can see the resonance structures of compound **1b** – in addition to the same one of compound **1a** – involving the aromatic cycle.*

Different experimental conditions were used in order to test the racemization potential of compound **2b** (ester). The first conditions were implemented in 7:3 proportion of acetonitrile and water by using **LiOD** – as our base – with final pH equal to 8 and 11. However, we noticed no changes in the alpha hydrogen peak since the experimental conditions might have been too mild.

The second conditions were realized by implementing the following proportions of acetonitrile and water respectively: 7:3, 8:2, 9:1 and 95:5. **DBU** was selected as the base (Spectra 1-4).

Considering the rate of **hydrogen-deuterium exchange**, we can clearly see from the graph below (Figure 22) that the H/D exchange increases with decreasing water content in the solution. Hence the experimental condition that shows the lower racemization is the 7:3 proportion, in which – after 21 days – we observe that 68% of compound **2b** had exchanged the alpha hydrogen with deuterium in solution.

The NMR tube with the lowest presence of water – 95:5 proportion – showed the highest rate of H/D exchange with a 92% displacement after 21 days (Spectrum 4). Almost the same percentage has been reached by 9:1 proportion although requiring more time (Spectrum 3). We can conclude that the **95:5** proportion is the best condition from the point of view of H/D exchange.

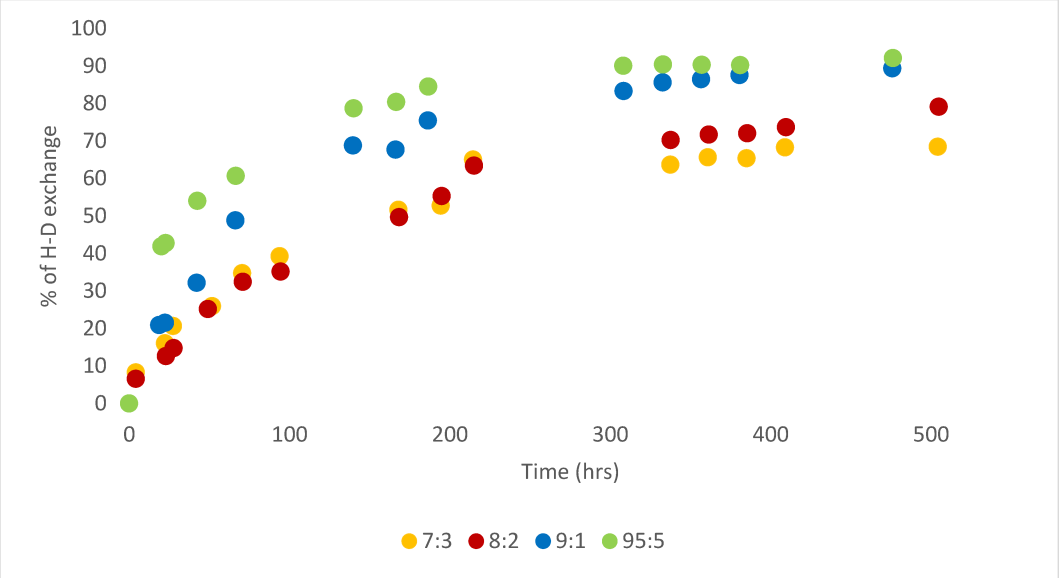

Figure 22. Graph showing the rate of racemization in all the four conditions that were realized.

However, the **hydrolysis** of the methyl ester group was observed too. the rates show an inverse trend in comparison to the one seen in the H/D exchange; as the H/D exchange increases with decreasing water in the solution, the hydrolysis rate decreased with decreasing amount of water. Ester hydrolysis occurs because of the presence of water in the solution, driving a nucleophile attack on the ester moiety (Figure 23A). This process emerged from the decrease in the integral value of methyl group at 3.66 ppm and the increase of integral value of methanol at 3.27 ppm (in 7:3 proportion).

In the graph below (figure 23B) we can see the rates of hydrolysis that were registered for 21 days. The experimental condition showing the highest grade of hydrolysis is the 7:3 proportion of the solvent mixture. In this case, 39% of compound **2b** present in the solution had been hydrolysed. For the 8:2 proportion, we have an increase in the hydrolysis up to 21%, and this

percentage is further reduced if we observe the 9:1 proportion, in which the amount of hydrolysis after 21 days reached 12% only. The lowest grade of hydrolysis is registered for the **95:5** proportion. In the latter condition we observe just a small number of molecules undergoing hydrolysis that reached the 4% only at the end of the recordings.

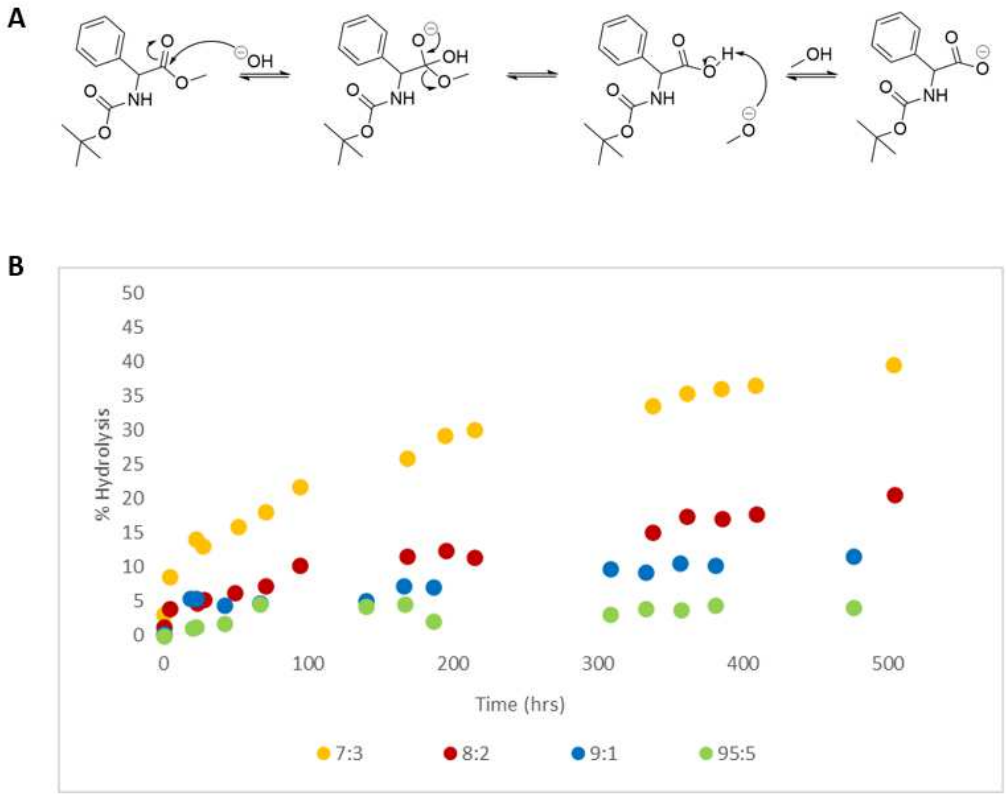

*Figure 23. (A) Reaction of hydrolysis in a basic environment. (B) Graph showing the kinetic of hydrolysis of compound **2b** methyl group, at different proportion of acetonitrile and water. The increase in hydrolysis is represented here by the reduction of methyl signal.*

We can consequently explain the increase in the rate of racemization with the decreased presence of **water** in solution, taking into consideration the decrease in the hydrolysis rate too. Higher hydrolysis rates lead to a higher fraction of acids in solution, and because these acids do not racemize this reduces the racemization rate.

Despite the previous studies showed that the ester can racemize, we failed to see H/D exchange on the acid form. It is reminded that racemization of the acids is essential to complete our reaction cycle. We tried to induce acid racemization by increasing the reaction **temperature**. In that way we might enhance the reactivity of all the compounds present in solution because of the increase in thermal movement in agreement with the Arrhenius equation

$$k = Ae^{-\frac{Ea}{RT}}$$

In our studies at higher temperature, we obtained, as expected, a much faster racemization of the **ester** that reached plateau in less than three hours (Figure 24A), in comparison to almost three weeks for experiments carried out at room temperature at 95:5 acetonitrile:D_2O medium. However, we also observed a huge increase in the hydrolysis rate (Figure 24B).

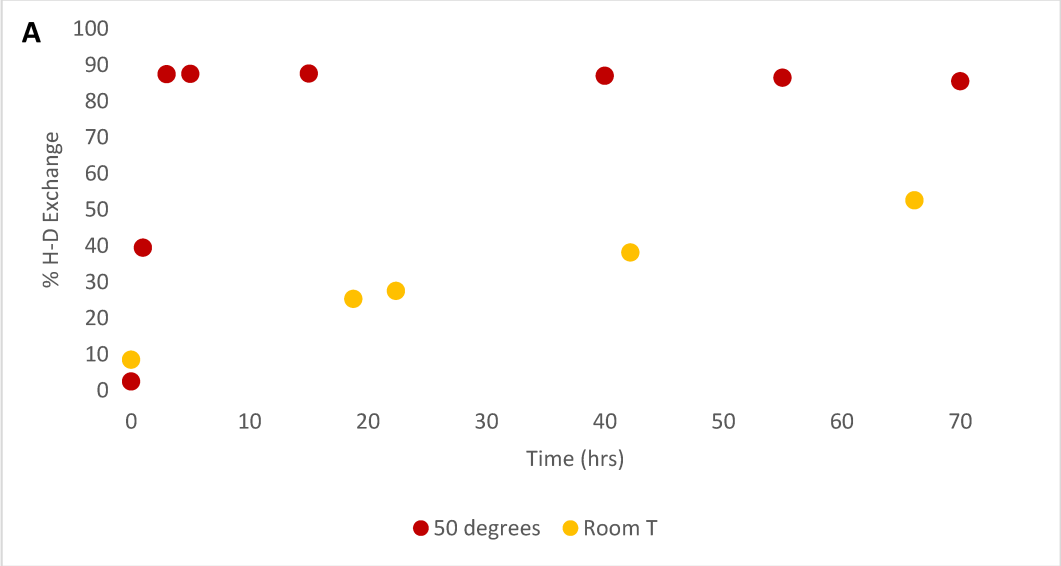

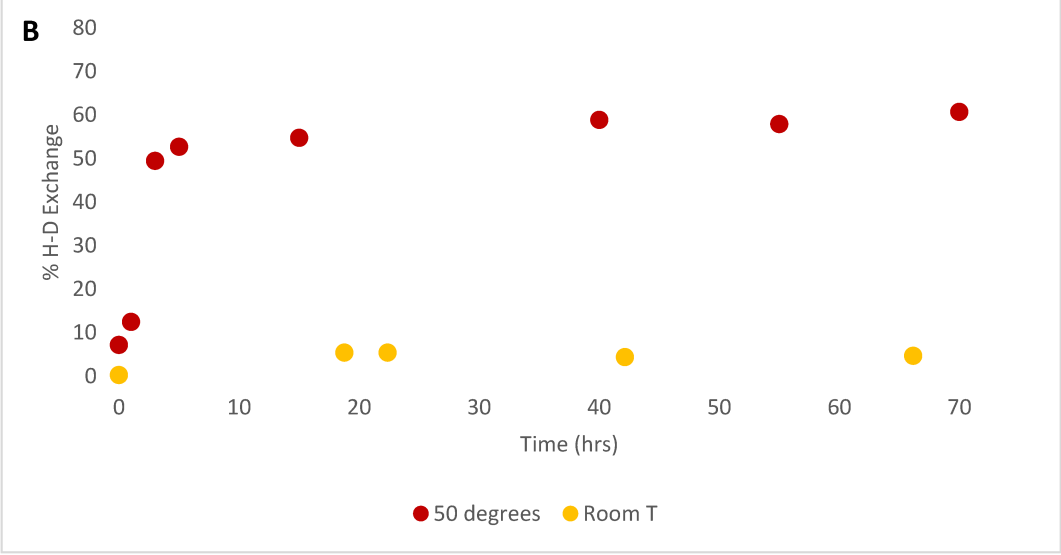

Figure 24.(A) Graph showing the kinetic of hydrogen-deuterium exchange in the tube placed at room T (yellow) and in the tube placed at 50 degrees (red). They both contain DBU and 9:1 proportion of acetonitrile and water respectively. (B) Graph showing the kinetic of hydrolysis in the tube placed at 50 degrees and in the tube placed at room T. They contain DBU and 9:1 proportion of acetonitrile and water respectively.

As we can see from the graphs above, at room temperature the hydrolysis is nearly absent. Instead, at 50 degrees we can clearly see a faster hydrogen-deuterium exchange, that shows a steep increase in the first few hours of recording. After that, the value is kept constant because of the presence of the acid species that subtract reagents to this reaction.

The **acid** form, instead, still showed no racemization even at 50 degrees. It means that we must move to another candidate.

3.4. RACEMIZATION STUDIES: COMPOUND 3

Considering the very low rate of H/D exchange of the acidic form of compound **2** we tried to improve it by replacing the N-Boc group with an EWG-group. We selected as best candidate the **trimethylammonium** group [27]. It is known to be a strong EWG-group because of the permanent positive charge on the nitrogen that might stabilize the negative charge developing on C-alfa upon racemization (Figure 19).

This new compound differs from the previous one because of the presence of the positively charged **ammonium group** (Figure 25). The two electron withdrawing groups – trimethylammonium with a net positive charge and phenyl group with aromatic properties – are both contributing to the stabilization of the carbanion intermediate that would form after the removal of the hydrogen from the chiral center. With this structural modification we could increase the alpha carbon acidity. However, we need to verify if it is enough for our purpose and in the experimental conditions we are implementing.

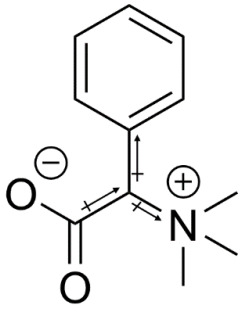

Figure 25. Scheme of the new compound in the acidic form. Here we have highlighted the electron withdrawing groups (trimethylammonium and aromatic cycle) and electron donating group (carboxylic acid).

Using this compound in the ester form, we have changed the solution composition by reducing the amount of organic phase, in order to avoid precipitation issues. In this case we abandoned the use of DBU and we regulated the pH through the use of phosphate and borate **buffers** in order to have the solution pH at the value of 7, 8, 9, 11.

We first explored the ester reactivity toward hydrolysis and H/D exchange in D_2O as solvent (figure 26, 27). Importantly, exchange occurs very fast at pH 11, in fact within 5 minutes the signal of alpha proton disappears. At pH 8 and 9 exchange occurred slower and we could follow the kinetics. Still, within one day in both conditions we observed the total disappearance of alpha proton. The slowest hydrogen-deuterium exchange was observed at neutral conditions. Almost two weeks were required to reach complete exchange.

Hydrolysis of the ester moiety in compound **3b** is present too. At pH 11 the complete hydrolysis was observed after 50 hours. At pH 9, instead, the full hydrolysis was observed after 1 month, and finally at pH 7 and 8 this process is very slow with only the 4% and 20% of ester hydrolysed after 1 month respectively.

Comparing these two processes it is clear that the H/D exchange occurs faster than hydrolysis. Hence the results are in agreement with one of our initial purposes. However, since the rate of hydrolysis must be reduced to allow the action of the enantioselective catalyst, the best condition seems the one presenting pH 7.

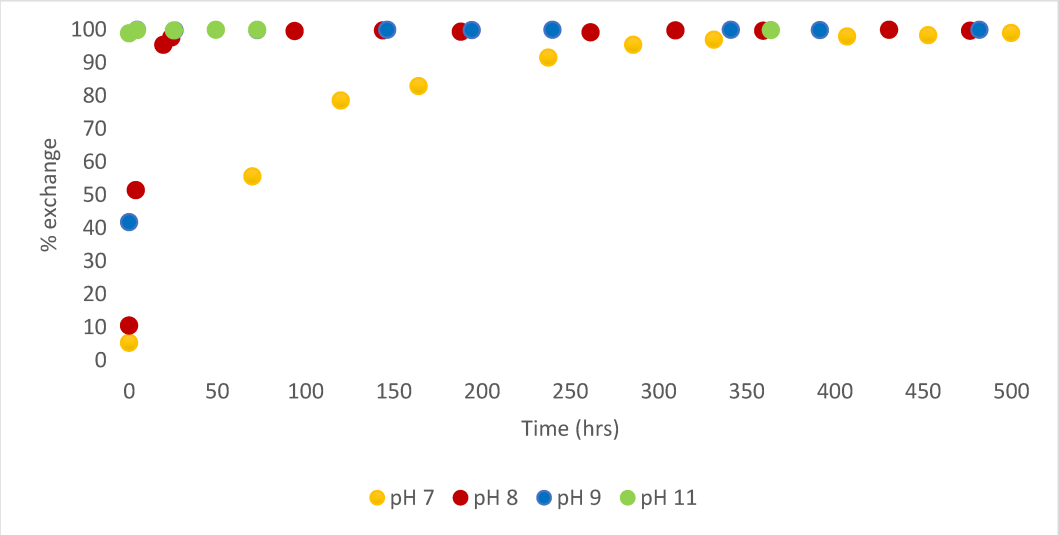

Figure 26. Graph showing the kinetic of hydrogen-deuterium exchange in full water, in all the four experimental conditions.

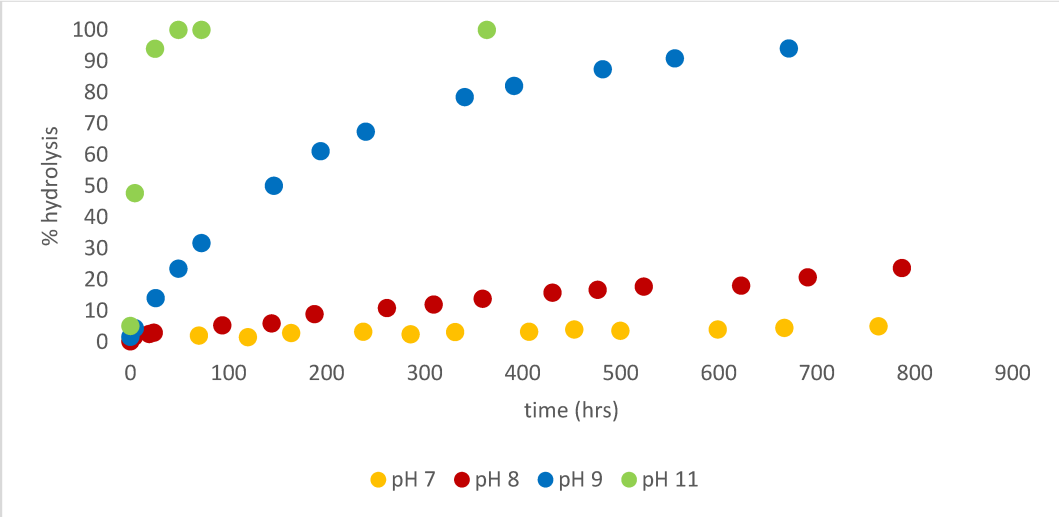

*Figure 27. Graphs related to kinetic of hydrolysis of compound **3b** placed in water, in all pH conditions.*

In the second set of experiments, we have used again all the different pH conditions, however we placed the samples in a mixture composed by 7 parts of water and **3 parts of acetonitrile** (Figure 28, Spectra 5-8).

The slowest rate of **H/D exchange** is still observed here at pH 7, reaching 92% of completion of the reaction after almost 5 days (Spectrum 5). At pH 8 full H/D exchange was achieved after almost 19 hours (Spectrum 6); instead, at pH 9 just 6 hours were required (Spectrum 7). The fastest exchange was observed under the most basic conditions (pH = 11) that showed an immediate exchange as soon as compound **3b** was placed in solution (Spectrum 8).

If we look at ester **hydrolysis kinetic**, the only NMR tube showing full hydrolysis is the one at pH 11. The others show a decreasing trend in the hydrolysis velocity, until pH 7 that reached the 5% of completion of it. In all cases, though, hydrolysis rates were much slower than racemization rates.

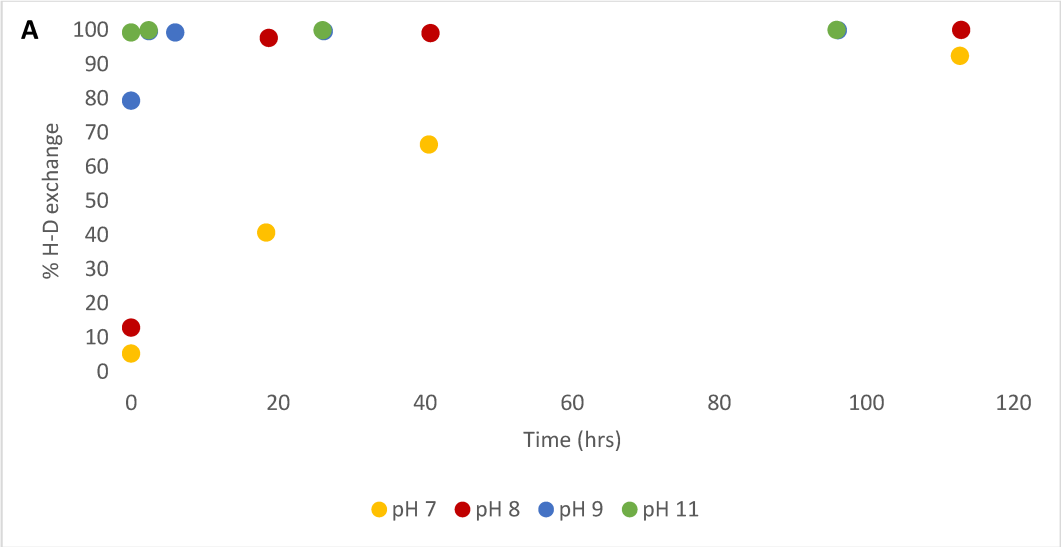

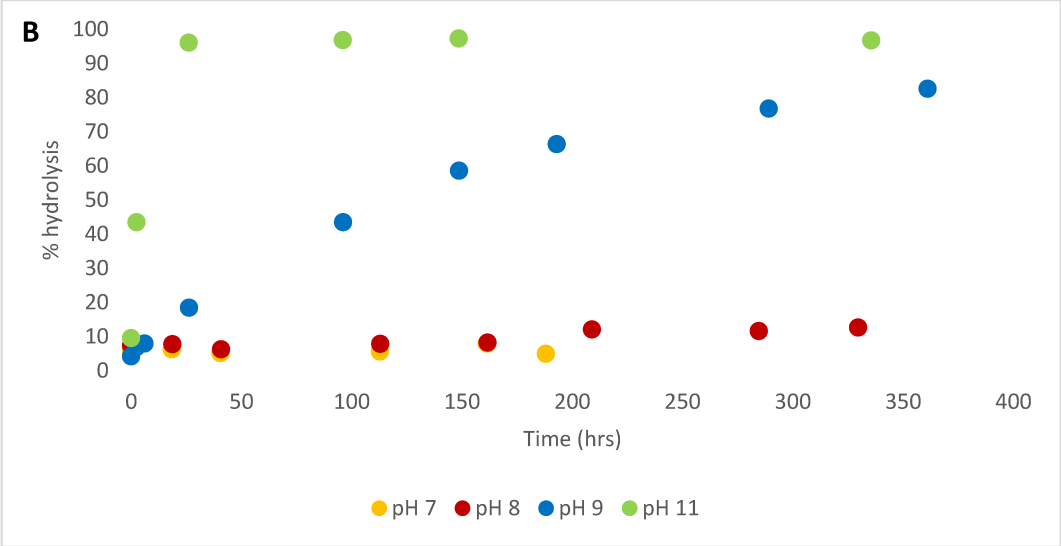

Figure 29. (A) Kinetic of hydrogen-deuterium exchange in the mixed solution. (B) Graphs related to kinetic of hydrolysis of compound 1c placed in a 7 to 3 proportion of water and acetonitrile.

To sum up, for compound **3b** in both conditions – full water and mixed solution – we can notice the same tendency connected to the **variation of pH**. Moving towards more basic environments – from pH 7 to pH 11 – we can see a clear increase in the racemization rate, and the same trend can be seen by observing the graphs related to the hydrolysis reaction.

Making a comparison between the tubes containing only water and the ones with mixed solution of acetonitrile and water, we can notice some changes in the rates related to racemization (Figure 29). This process is slightly faster in the mixed solution, and this can be clearly appreciated at pH 7 that shows the slower rate for this process.

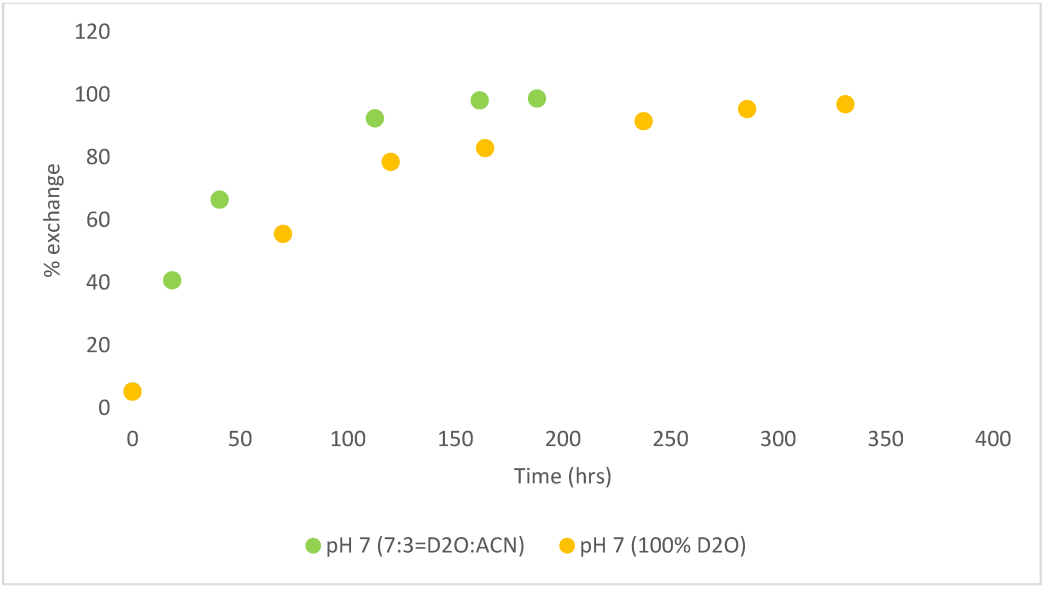

Figure 29. Kinetic comparison between exchange occurring at pH 7 in full water (yellow) and mixed solution (green).

Concerning the **acidic form**, since at room temperature we could see no racemization of the species in solution, we placed the acid containing tubes at 50 degrees to see if some changes might occur. In the case of a positive result, we might have thought about the possibility of creating a system characterized by different temperatures triggering different processes. Room temperature could have been used for the ester stage of the system. The increase in the temperature, instead, might have promoted the acid racemization. However, we were able to see just very slow racemization at pH 11 (figure 30). Despite the good and promising results obtained with ester form of **3** we were therefore not yet able to obtain a satisfying racemization of acid form.

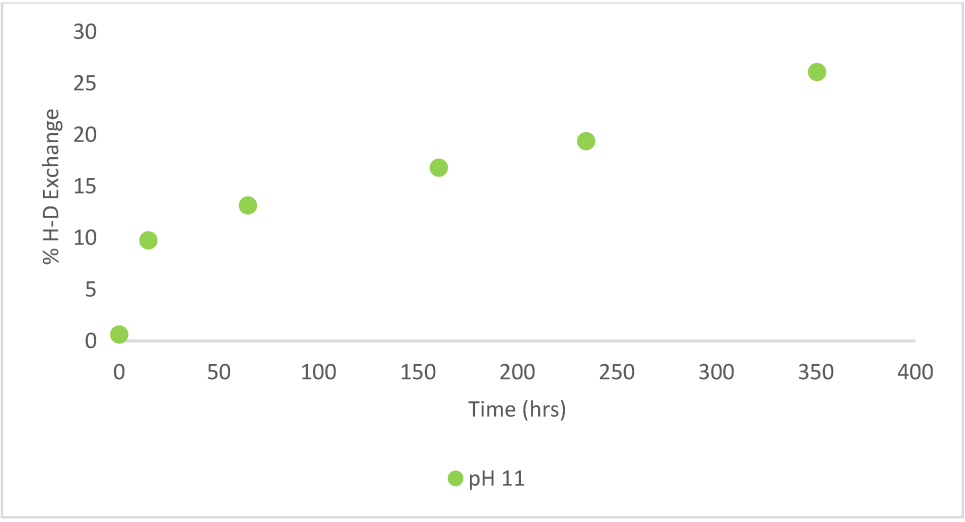

*Figure 30. Kinetic of racemization of compound **3a**, placed at 50 degrees.*

3.5. RACEMIZATION STUDIES: COMPOUND 4

The new compound synthesized is characterized by the replacement of the ammonium group with a **3-methyl imidazole unit**. It was hypothesized that the presence of this additional aromatic group would further delocalize negative charge of the intermediate (Figure 31).

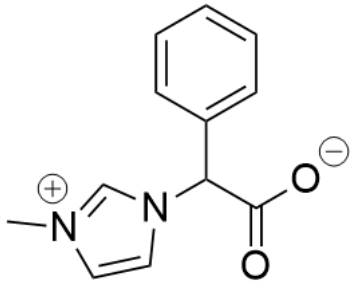

*Figure 31. Structure of compound **4a**.*

The increased acidic character of the alpha carbon emerged from the **chemical shift** of the hydrogen attached to C-alfa. The higher in ppm is the position of the target peak (downfield shift), the more the hydrogen nucleus is deshielded. The presence of electron withdrawing groups that deshield nearby hydrogen nuclei is the reason why the signal shifts to higher ppm values. [28].

For our purpose, the higher are the ppm associated to the hydrogen associated to the alpha carbon of the molecule, the more the nucleus is deshielded, which implies a higher acidity. For all compounds that we have studied, we have indeed observed that the alpha hydrogen peak position is at higher ppm values in the ester form compared to the acid. It is therefore highly informative for us to notice that the alpha hydrogen peak of compound **4** is located at higher ppm values compare to compound **3** (6.19 ppm for the first one, 4.94 ppm for the latter, both as acids). It suggests a higher acidity.

Racemization studies with compound 4 – both acid and ester – were performed using buffers that stabilize the pH at 7, 8, 9 and 11. The solution is composed by 7 parts of water and 3 parts of acetonitrile – both deuterated. We could not use exclusively water since the ester is not soluble.

Racemization of the **acidic form** was observed at pH 11 and reached completion after 9 hours at pH 11 (Figure 32A, Spectrum 11). Instead, at pH equal to 9, we have the 70% reduction in the signal coming from the alpha hydrogen after almost two weeks (Spectrum 10). On the other hand, only little changes were recorded at pH 8 and 7 (Figure 32B, Spectrum 9).

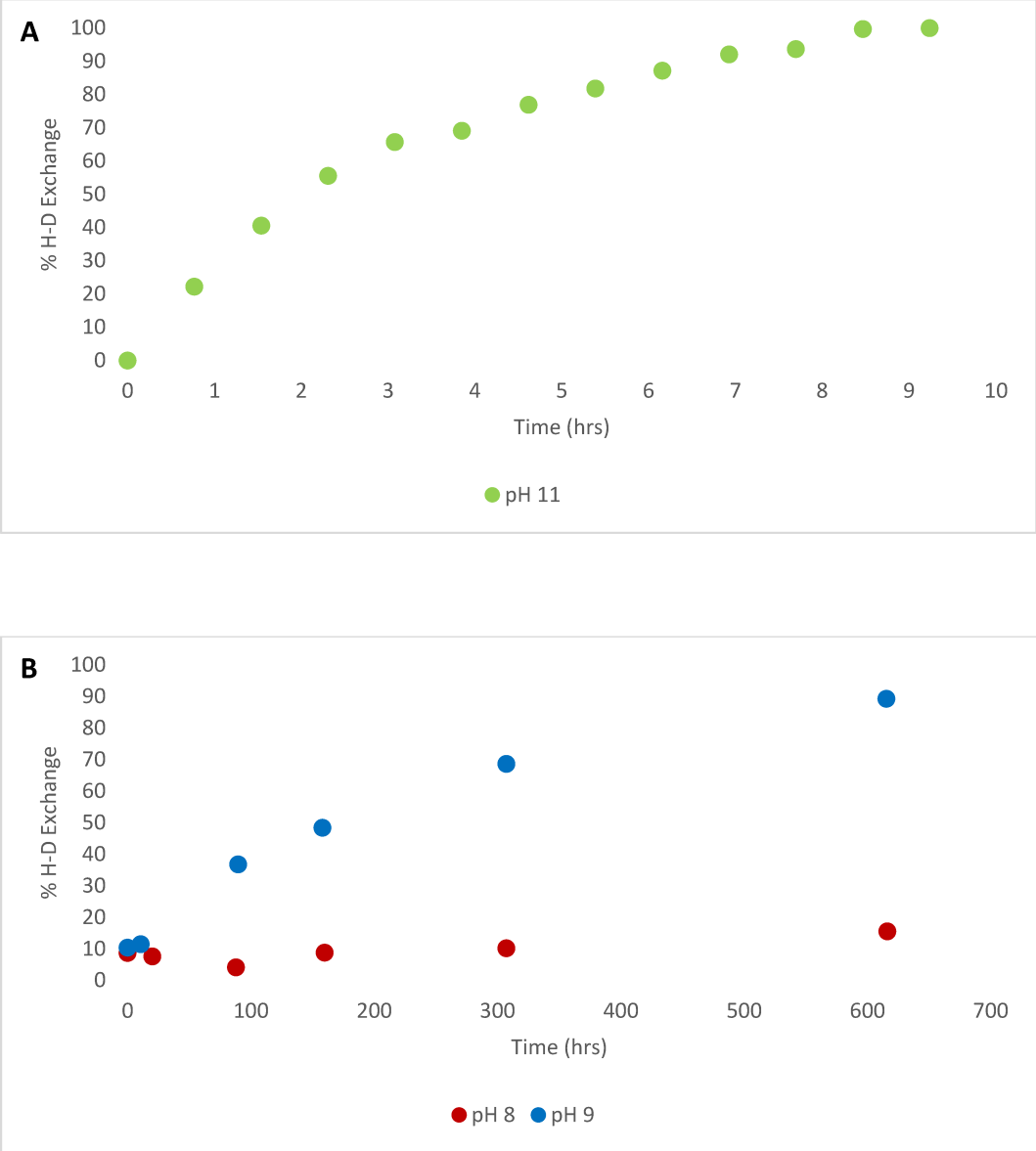

Figure 32. (A) Kinetic of compound 4a racemization at pH 11. (B) Kinetic of racemization of the acidic form of compound 4a at pH 8 and 9.

The racemization of the acid that we obtained here is a promising result, and it means that the increase in the acidity of alpha hydrogen was effective. Thus, we shifted our attention to the study of the **ethyl-ester** that – based on the observation of compound 2 and 3 – should have a very fast rate of racemization. Unfortunately, it turns out that this molecule is not stable in solution and degrades as soon as it solubilised (Figure 33). As seen below after 2 hours despite the disappearance of the signal of the proton attached to C-alfa, we observe changes in the spectrum – especially in the aromatic area – that suggest structural instability.

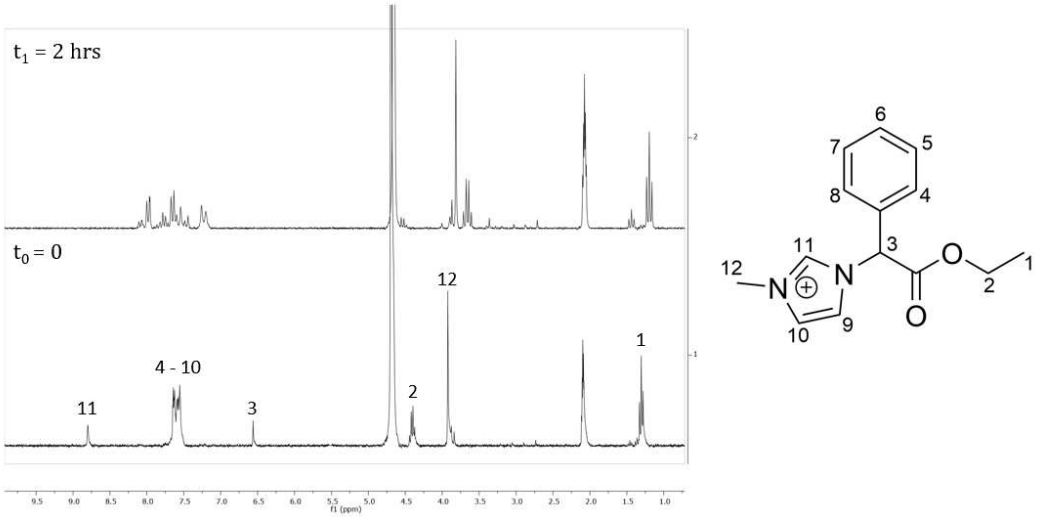

*Figure 33. Spectrum at time zero (below) and after two hours (above) of the tube containing compound **4b** in 5:5 proportion of acetonitrile and water, at pH 7.*

3.6. ESTERIFICATION STUDIES

From the results obtained in the racemization studies, we have therefore selected the **compound 3** to be used for further studies. It can give a quite fast and efficient racemization of the ester even under mild conditions (pH 7 and 25°C), it is stable both as acid and as ester, and it could give H/D exchange of the acid form too, at pH 11 and 50°C. Since the racemization of acid **3a** was observed only at extreme conditions of pH and temperature, we decided to construct a partial system that would allow chemically fuelled enantiomeric enrichment but lacking the possibility to racemise after fuel depletion. What is needed for this to work is an activation step to convert the acid into ester, the corresponding racemization of the ester and the final hydrolysis of the ester back to the acid.

The following studies concern, in particular, the passage of our compound from the acid state (inactive) to the ester state (active) thanks to the presence of a **chemical fuel** in the solution. This step is fundamental because it leads to the formation of an activated compound that is able to perform dynamic kinetic resolution, driving in the end the system out of equilibrium. We have consequently tested the efficacy of different chemical fuels and experimental conditions for the esterification of compound **3a**.

Some research in the scientific literature helped us in finding the most suitable chemical fuels for our research.

3.7. ESTERIFICATION STUDIES: METHYL IODIDE

The first chemical fuel that was used for activation studies on compound **3a** is methyl iodide (**MeI**) and it was chosen on the basis of the system described by Job Boekhoven et al. [6]. In that system MeI was used to activate the monomers and trigger the self-assembly (see introduction). It is the simplest chemical fuel that can be implemented for these studies, and it would act transforming the carboxylic acid into a methyl ester (Figure 35).

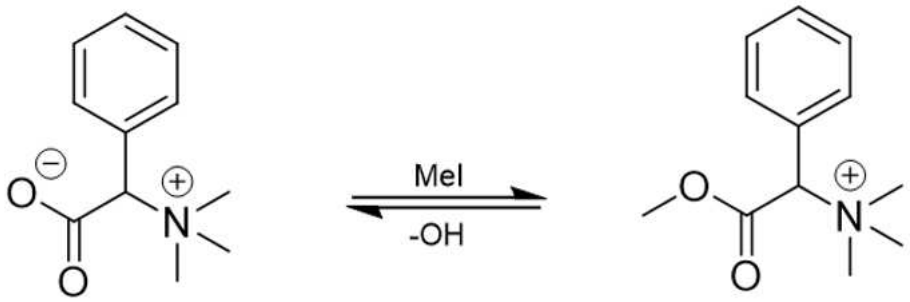

*Figure 34. Activation reaction of compound **3a** with methyl iodide.*

This chemical fuel would not be able to give us the additional chiral site that we required. However, these explorative studies would be useful for the implementation – in the future – of new chiral fuels that would present the right structure to give the **first directionality bias** for our system.

These analyses were performed with different equivalents of the chemical fuel and maintaining pH 7 through buffer or adjusting with NaOD. Yet, in none of the conditions studied we could find trace of ester. Rather, we observed a hydrolysis of methyl iodide to methanol.

3.8. ESTERIFICATION STUDIES: EDC and NHS

The following activation studies were performed by adapting a procedure that is usually adopted for carboxylic acids amination and crosslinking to surfaces [29, 30, 31]. It can be realized by using in combination the well-known activating agent 1-ethyl-3-(-3-dimethylaminopropyl) carbodiimide (**EDC**) together with N-hydroxysuccinimide (**NHS**).

The reaction involves nucleophilic attack by the carboxylic moiety of compound **3** to EDC forming the **O-acylisourea** intermediate. This coupling product is highly instable; however, it reacts quickly with NHS leading to the formation of the hydroxyimide-ester and release of urea. The latter coupling – NHS plus compound **3a** – is stable enough at the desired pH (NHS esters have a half-life of 4-5 hours at pH 7, that decreased with the increase of basicity

[29]). This ester should therefore theoretically be able to perform the remaining steps of our cyclic system: in particular racemization of the ester followed by hydrolysis to complete the dynamic kinetic resolution procedure (Figure 35).

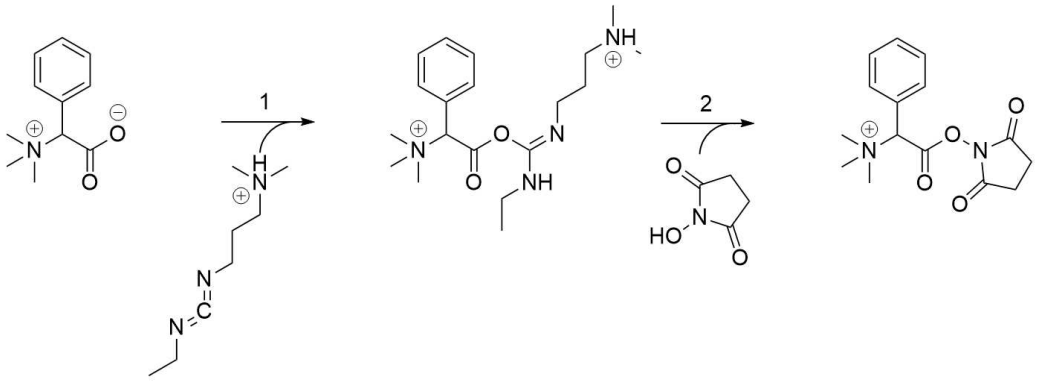

*Figure 35. Mechanism of activation mediated by EDC and NHS. The first step is characterized by the attachment of EDC to compound **3a** at the C-terminus. It triggers the attachment of NHS to the same site, thus forming a stable ester (step 2) and releasing isourea (the waste of this reaction).*

We tested multiple experimental conditions by changing the composition of the solution and the concentration of the activating compounds. However, we were able to observe the transformation of EDC into isourea only. In particular, we observed that the EDC alone is stable in the designed experimental conditions, and it remains stable after the addition of compound 3a in the solution too. On the other hand, as soon as NHS is added, we see isourea formation that is clearly identified by the appearance of new signals of the methyl group at lower ppm (Figure 36).

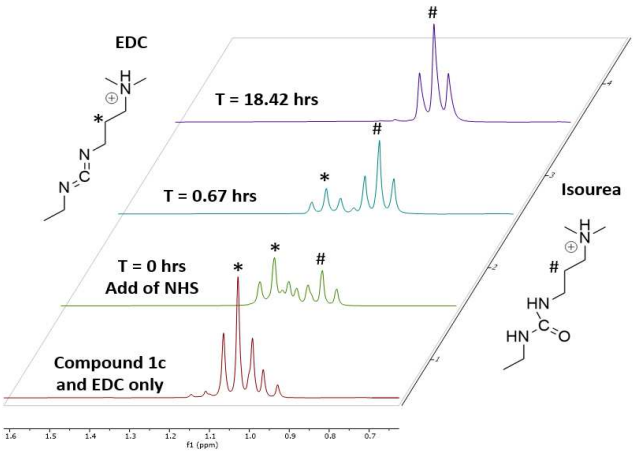

*Figure 36. We have here the spectra recorded of the sample containing EDC, compound **3a** and NHS. In particular, this is the triplet representing the -CH_2 that is located in the most apolar region of our molecule.*

We could never detect either the presence of the ester form of **3** in solution or the reduction of the alpha hydrogen peak. This means that the coupling was not effective, and the racemization was not triggered by the experimental conditions implemented here.

3.9. ESTERIFICATION STUDIES: DIC and NHS

We decided to change carbodiimide and employ as activating agent *N*,*N*′-diisopropylcarbodiimide (**DIC**). Despite its great disadvantage because of the insolubility of the waste product, it has been already employed in many dissipative systems [10].

The NMR tube implemented in this case contained the three components needed for the reaction of activation, **DIC, NHS and compound 3a**. 1 equivalent of **3a** (0.01 M) together with 10 equivalents of NHS and 10 equivalents of DIC was placed in a mixture of 5 to 5 equivalents of acetonitrile and water, and the pH was selected to be equal to 5 since it is known that slight acidic values would promote the coupling between DIC and carboxylic acids [29]. After a night of recording, we registered some changes in the spectra obtained.

We can see from the kinetic analysis that after almost 22 hours, the alpha hydrogen peak was reduced by 36% (Figure 37A). The H/D exchange reached a plateau when complete consumption of the chemical fuel had taken place. We observed furthermore the reduction in NHS peak and changes in DIC peaks position that corresponded to the formation of isourea in solution. This observation seems to suggest that the activation worked, and that H/D exchange could occur only if the chemical fuel is still present in the solution. In fact, it was observed that further addition of the fuel together with DIC caused a subsequent increase in the H/D exchange of the 23% (Figure 37B).

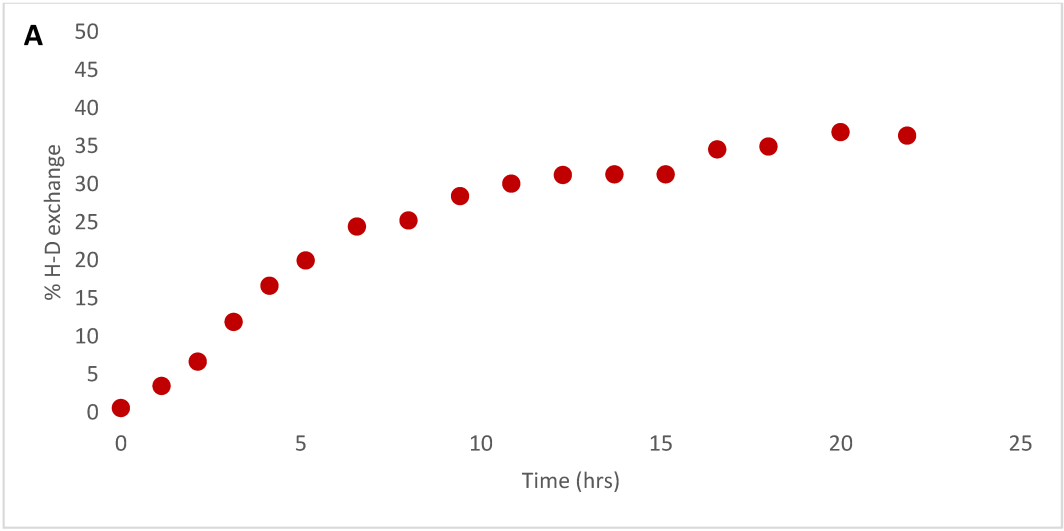

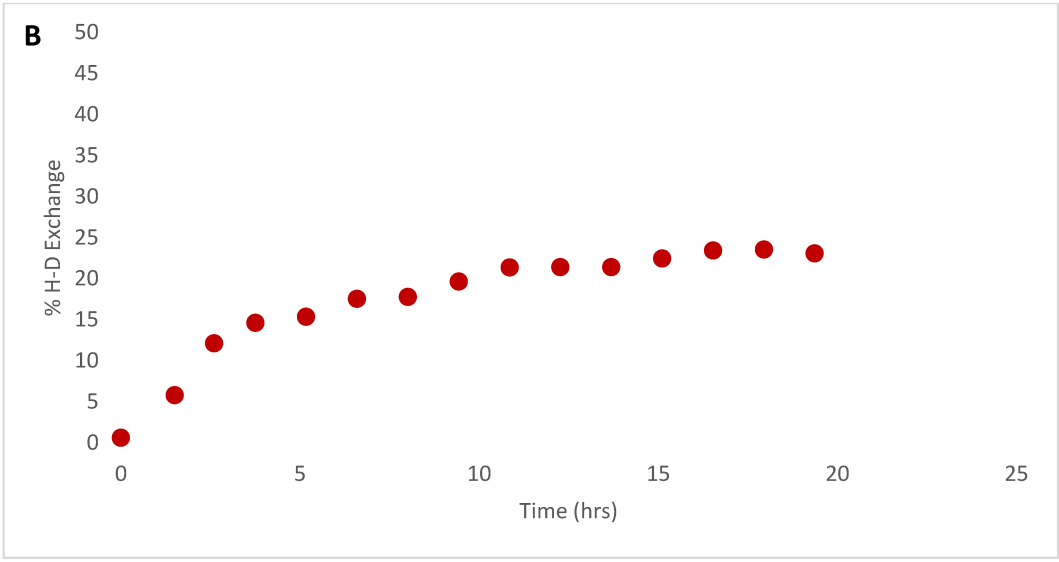

*Figure 37. (A) Kinetic of hydrogen-deuterium exchange of the alpha hydrogen of **3a** placed in solution with NHS and DIC. (B) Kinetic of hydrogen-deuterium exchange of **3a** after addition of ten more equivalents of DIC and NHS.*

However, signals corresponding to the ester of compound **3** were never observed. Yet, since we have seen from previous studies that the acid form of **3** is not able to racemize under these acidic conditions, we thought that the reduction in the intensity of the hydrogen signal of C-alfa might be due to other processes occurring in solution.

Therefore, we verified the **stability** of each component under the same experimental conditions. First of all, we placed DIC alone in 5:5 acetonitrile water at pH 5. Our chemical fuel showed no changes in these conditions; it means that the water alone cannot give its transformation into isourea.

Further verifications were done by placing in solution **compound 3a with DIC**, to see if that molecule can catalyse hydration of the carbodiimide. Following the coupling reaction seen before (Figure 35), DIC should be the first component to react with the carboxylic moiety of our amino acid. It would detach upon reaction of the activated ester with NHS and release isourea. However, nothing changed in the peaks associated with DIC and in the ones associated with **3a**. This observation led us to the conclusion that there is no reaction between these two molecules.

The tube containing **NHS and compound 3a** was studied too, to verify if NHS alone can form a stable ester with our amino acid derivative. We did not observe any shift in the C-alfa hydrogen signal indicating that the ester did not form. Consequently, we deduce that, at least, the presence of DIC in solution is required. The last combination introduced is the one comprising **NHS and DIC only** to see if they react with each other and if some changes might occur in solution. Indeed, we could observe the complete transformation of DIC into the waste compound (Figure 38A). What is more, by comparing the rate of this transformation with the one occurred in the tube composed by all the three elements in solution, we can see that they are highly comparable (Figure 38B). This finding made us think that the activation of compound **3a** can be due to other processes or reactions happening inside the tube.

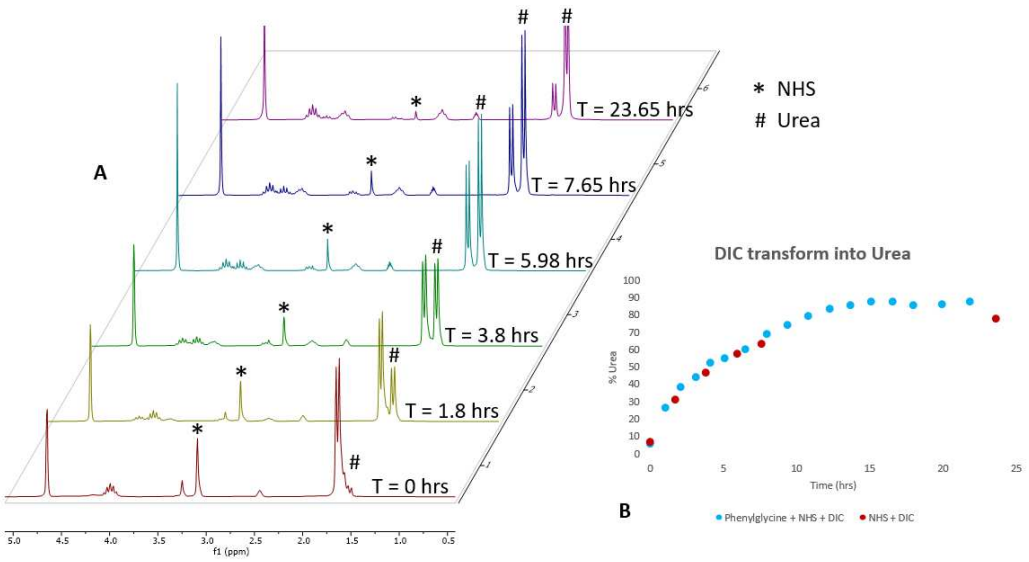

Figure 38. (A) Spectra of the sample composed by NHS and DIC. From time zero to the latter, we observe an increase in the urea presence. (B) Kinetic representing the transformation from DIC to Urea in the complete sample (light blue) and in the sample containing NHS and DIC only (red).

Since NHS is responsible for the transformation of DIC into urea, we investigated which compound and/or process could be responsible for the hydrogen-deuterium exchange at the alpha carbon site of compound **3a**. We had already seen that **3a** together with NHS only and DIC only, produced no

changes in the target signal or any other change in the elements that are present in solution. For this reason, we have added in solution our amino acid together with **isourea**, to see if the waste formation would have been responsible for the acid activation. However, we could record no changes in the peaks associated to our target after four days of recording.

4. CONCLUSIONS

The objective of this thesis project was to develop an out-of-equilibrium system, where a fuel was used to drive the deracemization of a racemic mixture. We started our studies from the most relevant chiral compounds present in nature: amino acids. The objective was to activate them for racemization through the formation of an amino ester using a chiral carbodiimide or a chiral alkyl iodide. Racemization conditions were studied by following H/D exchange via NMR spectroscopy. The first amino acid that showed an appreciable H/D exchange was ***N*-Boc phenylglycine methyl ester**, that was complete in 20 days in 95:5 $ACNd_3$:D_2O using DBU as base at a pH of around 13. Anyway, phenylglycine acid form didn't show racemization even after prolonged heating at 50 °C. Thus, we decided to improve the acidity of phenylglycine substituting the N-Boc with a more electron-withdrawing **trimethylammonium** group. This molecule shows fast racemization of alpha proton at mild condition (14 days at pH=7.0) but even in this case we were not able to see H/D exchange of the acid. A further optimization of the structure concerned the insertion of **3-methyl imidazole** at the place of the ammonium group. In this case the data regarding the acid were promising. We were able to detece fast racemization that reached completion after 9 hours at pH 11 and 90% of reduction after 25 days at pH 9. Despite these promising observations, the related ethyl ester of this compound was found to be not stable in solution and degraded very fast.

Concerning the esterification studies, we take as model molecule for our analysis compound **3a**, even if we were aware that this compound as carboxylic acid didn't show racemization. Different experimental conditions were tested to drive the activation of the starting compound and consequent dynamic kinetic resolution process. Indeed, we found that **DIC** seems the most promising chemical fuel since we observed the reduction in the hydrogen signal of C-alfa when both DIC and NHS were present. Yet, we were unable to convincingly show that this decrease resulted from the formation of the ester form of compound **3**.

In the future, based on the studies of this thesis, further attempts will be made in order to find an amino acid derivative who shows a fast enough racemization rate. By the way, we are open to explore other possible candidate molecules with a fast enough racemization rate, between them hidantoins or derivatives of malonic esters derivatives are the most likely. In addition, we will figure out the mechanism with whom DIC is active toward the racemization of compound 3a, whose mechanism looks very different compared the one reported in literature.

The next step would be to prove that racemization occurs starting from enantiopure compounds. Different techniques would be used to better characterize what is occurring in solution, between them the most suitable are **circular dichroism** and polarimetry. Since the compounds that have been used so far presented an aromatic site on them, they can emit a signal strong

enough to be recorded. The difference in absorbance of the molecule can be correlated to the enantiomeric composition of the solution [34].

The long-term goal of this studies is the development of a catalyst such as a **proline**-analogue that is able to be transiently deracemized throughout this pathway. In this fashion, using the catalytic properties of proline, we would be able to transiently catalyse enantioselective a reaction that is switched on and off by addition of a fuel (Figure 39). This is actually what happens in living organisms, in which every process is highly interconnected with all the others, and nothing is left to chance. Indeed, we think that it will be a step forward toward the comprehension of how chirality appeared in the earth.

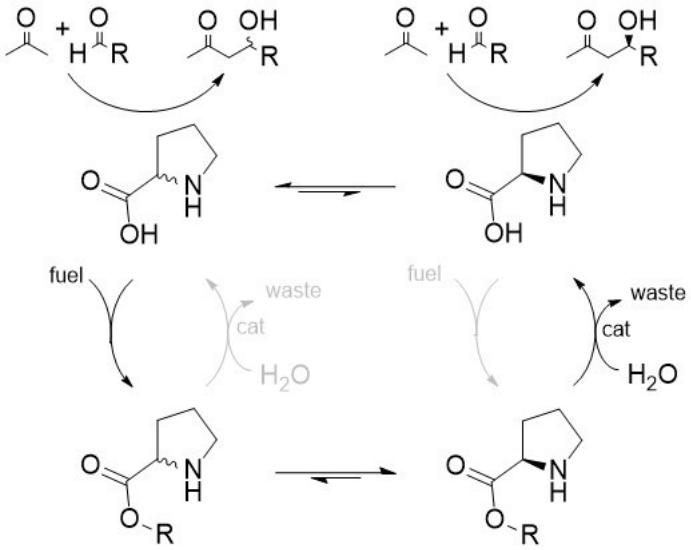

Figure 39. Cyclic system presented before with proline instead of the compounds we used. Above we can see a possible reaction that is catalysed by proline, here a direct aldol reaction. On the left the catalyst is the proline racemate, thus a racemate in the parallel reaction is obtained too. On the right, instead, the catalyst is an enantiopure proline, consequently an enantiopure solution is obtained in the parallel reaction too.

5. MATERIALS and METHODS

5.1. GENERAL

The reagents and materials used in the synthesis of the compounds described below were bought from commercial sources, without purification. Anhydrous solvents were used without further purification. NMR spectra were recorded using commercially available deuterated solvents. Flash column chromatography was performed using silica gel 60 (Aldrich) and a suitable eluent. Analytical TLC was performed on aluminium backed plates pre-coated (0.25 mm) with Macherey-Nagel Alugram® Xtra SIL G/UV254 with a suitable solvent system and was visualized using UV fluorescence (254 nm) and/or developed with ninhydrin, phosphomolybdic acid (PMA), potassium permanganate. Potassium Hydrogen phosphate dibasic and boric acid were purchased from Sigma-Aldrich and used without further purification. The pH of buffer solution (7.20) was determined at room temperature using a Metrohm-632 pH-meter equipped with an Ag/AgCl/KCl reference electrode. All NMR spectra were recorded on a Bruker Avance 300 UltraShield, or Bruker Avance 200 spectrometer using the residual solvent as the internal standard. All chemical shifts (δ) are quoted in ppm and coupling constants given in Hz. Splitting patterns are given as follows: s (singlet), d (doublet), t (triplet), q (quadruplet), p(pentaplet), m (multiplet).

5.2. SYNTHESIS

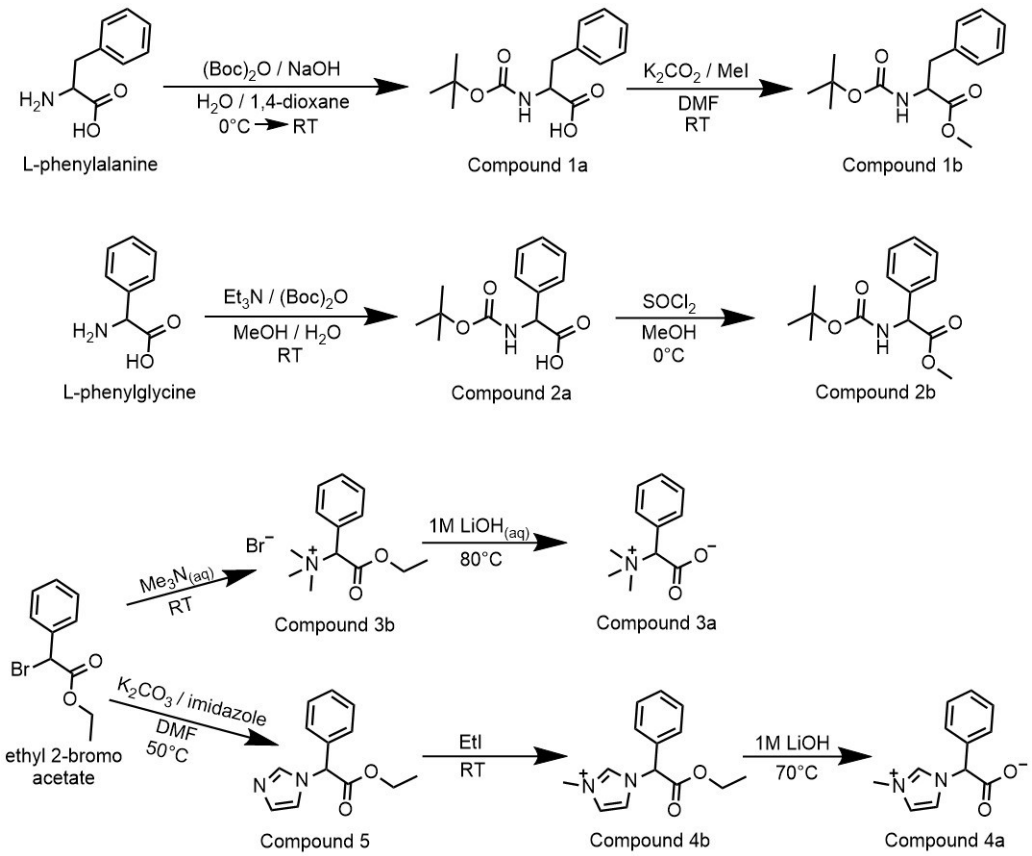

Figure 40. General scheme of the synthesis of compounds used in this project.

Compound 1a: 1 equivalent of L-phenylalanine (1.65 g) was dissolved in a mixture composed by 10 mL of NaOH, 10 mL of water and 20 mL of 1,4-dioxane. After that the solution was cooled to 0°C. 1.1 equivalent of di-tert-buthyl dicarbonate (2.20 g, boc anhydride) was added to the solution that then was stirred for 10 hrs at room temperature. After 3 days some free L-phenylalanine was still present in solution, thus we added other 1.1 equivalents of Boc-anhydride. Four hours later the volume of the solution was reduced to one third under vacuum. Saturated $KHSO_4$ solution was used to acidify the reaction mixture and later the aqueous layer was extracted with ethyl acetate (3 x 40 mL). The sample was further cleaned up with a chromatographic column to remove the remaining boc anhydride and then dried under vacuum. [31] ^{1} H NMR (300 MHz, CDCl3): d = 1.54 (s, 9H), 7.00 (dd, J = 8, 4.7 Hz, 1H), 7.32 (dd, J = 8, 1.5 Hz, 1H), 7.91 (dd, J = 4.7, 1.5 Hz, 1H), 9.31 (s, 1H, OH), 9.96 (br s, 1H, NH); 13C NMR (75 MHz, CDCl3): d = 28.2 (CH3), 83.1 (C), 121.2 (CH), 127.8 (CH), 138.8 (CH), 140.3 (C), 143.8 (C), 156.1 (C=O);

Compound 1b: 1 equivalent of compound 1a (3.00 g) and 3 equivalents of K_2CO_2 (4.68 g) were added to a solution of DMF (40 mL). After 2 hours of stirring at room temperature, 3 equivalents of iodomethane (2.11 mL) were added to the solution and the stirring continued for other 24 hours [32]. To separate our compound from DMF we added LiCl 5% to the solution and ethyl acetate, thus performing an extraction. The mixture was placed under vacuum to let the remaining solvent evaporate. ^{1}H NMR (400 MHz, CDCI3) δ 7.27 (5H, m, ArCH), 7.08 (1 H, br s, -NH-), 4.94 (0.6H, s, NHCH), 4.53 (0.4H, s, NHCH), 3.62 (3H, s, COOCH3), 3.04 (2H, m, ArCH2COOCH3), 1.38 (9H, s, HN-COOC(CH3)3); 3C NMR (100 MHz, CDCI3) δ 172.55 (COOCH3), 155.40 (NC(0)OC(CH3)3), 136.44 (quaternary C), 129.44 (ArCH), 128.69 (ArCH), 127.27 (ArCH), 76.85 (C(CH3)3), 54.63 (CH2CHC(0)OCH3), 51.68 (OCH3), 38.46 (CH2), 27.18 (C(CH3)3)

Compound 2a: The L- phenylglycine (1.51g, 10mmol) was placed in a reaction flask was added 20mL of methanol: water (3: 1), room temperature. Et_3N (1.51mL, 15mmol) was added, then $(Boc)_2O$ (3.27g, 15mmol) was added dropwise to the reaction mixture. The resulting mixture was stirred at room temperature overnight, the solvent was removed by rotary evaporation, dissolved in 100mL of citric acid, with acetic acid ethyl ester (3 × 50mL) and extracted with anhydrous sodium sulphate. (1.9g, 72% yield)

Compound 2b: To a stirring solution of compound 2a (500mg, 2mmol, 1eq.) in 20mL of Methanol at 0°C was added dropwise 175uL of $SOCl_2$ (285mg, 2.4mmol, 1.2 eq.). The resulting suspension was stirred at reflux for 16hrs. The reaction was followed by TLC (eluent EtOAc:PE 9:1). When the starting compound disappear remove the solvent under vacuum and use the compound without further purification. (Yield:505mg, 95%) ^{1}H NMR ($CDCl_3$) δ 1.41 (s, 9H), 3.73 (s, 3H), 5.34 (d, 1H, *J* = 7.3 Hz), 5.55 (d, 1H, *J* = 7.3 Hz), 7.30–7.44 (m, 5H); ^{13}C NMR ($CDCl_3$) δ 28.3, 52.7, 57.5, 79.90, 127.2, 128.6, 129.1, 137.0, 154.8, 171.6.

Compound 3b: To a 15mL solution of 40% trimethylamine in water add 1.22gr of ethyl 2-phenyl 2-bromo acetate (5mmol). Stir the solution at RT for 1 day. A white precipitate appears. Remove under nitrogen flux the excess of trimethylamine and the under vacuum the residual water. Use the compound without any further purification. (Yield: 1.5gr, 98%) ^{1}H NMR (400 MHz, Deuterium Oxide) δ 7.69 – 7.44 (m, 5H), 5.43 (s, 1H), 4.37 – 4.12 (m, 2H), 3.11 (s, 9H), 1.11 (t, J = 7.1 Hz, 3H). 13C NMR (101 MHz, D2O) δ 187.98, 167.28, 166.71, 131.89, 129.69, 126.00, 75.75, 63.94, 51.95, 12.88.

Compound 3a: Dissolve 0.5 gr of compound 3b (0.233mmol) in 5mL of LiOH 1M. Stir the solution at 80 °C for 12 hours. Remove water under vacuum, dissolve the solid in ethanol, centrifuge, recover the supernatant and dry it. (Yield: 0.175mg, 56%) ^{1}H NMR (400 MHz, Deuterium Oxide) δ 7.61 – 7.39 (m, 5H), 5.02 (s, 1H), 3.06(s, 9H). 13C NMR (101 MHz, D2O) δ 175.15, 165.2, 164.88, 130.29, 127.5, 125.25, 71.16, 49.73.

Compound 5: Dissolve in 1mL of DMF 1.22gr of ethyl 2-phenyl 2-bromo acetate (5mmol, 1eq.) add 680 mg of imidazole (10mmol, 2eq.) and 1.37 gr of K_2CO_3 (10mmol, 2eq.). Stir at 50 degree for 10 hours. Follow the reaction via TLC (Eluent: PE:EtOAc 3:7) Dissolve the reaction mixture in LiCl 5% and extract 3 times with Ethyl Acetate. Collect the organic phase and dry it with sodium sulphate. Remove the solvent under vacuum and purify via flash chromatography (PE:EtOAc 3:7 -> EtOAc 100%). Yield 747 mg, 63%. ^{1}H NMR (500 MHz, Chloroform-d) δ 7.63 (s, 1H), 7.45 – 7.36 (m, 3H), 7.34 – 7.30 (m, 2H), 7.06 (d, J = 18.0 Hz, 2H), 5.93 (s, 1H), 4.42 – 4.17 (q, 2H), 1.27 (t, J = 11.7 Hz 3H).

Compound 4b: In neat, mix 325 uL of methyl iodide (852mg, 6equiv.) and 230mg of compound 5 (1mmol, 1equiv.). Stir at room temperature overnight. Follow the reaction via TLC (eluent EtOAc:MeOH 95:5). Once reaction complete remove in vacuum the excess of Methyl Iodide. The compound was used without further purification. Yield assumed quantitative. ^{1}H NMR (400 MHz, Chloroform-d) δ 9.85 (d, J = 12.6 Hz, 1H), 7.63 (d, J = 1.9 Hz, 1H), 7.51 (dt, J = 7.1, 3.9 Hz, 2H), 7.47 (d, J = 1.9 Hz, 1H), 7.40 – 7.33 (m, 1H), 6.97 (d, J = 6.1 Hz, 1H), 4.32 – 4.09 (q, 2H), 3.99 (s, 3H), 1.17 (t, J = 7.1 Hz, 3H). 13C NMR (101 MHz, CDCl3) δ 167.14, 136.63, 136.54, 131.73, 129.84, 128.76, 123.60, 122.00, 63.43, 37.44, 13.97.

Compound 4a: To a solution 1M of LiOH dissolve 500mg of compound 4b. Stir at 70 °C for 16 hours. Remove the solvent under vacuum. Add ethanol to the solid and centrifuge the suspension. Repeat 3x, collect the supernatant and dry under vacuum. Yield: 357mg, 52% ^{1}H NMR (400 MHz, Deuterium Oxide) δ 8.47 (s, 1H), 7.50 – 7.41 (m, 5H), 7.35 (d, J = 1.7 Hz, 2H), 6.03 (s, 1H), 3.78 (s, 3H). 13C NMR (101 MHz, D2O) δ 173.10, 136.05, 133.63, 129.96, 129.68, 129.10, 123.17, 122.40, 67.71, 35.88.

5.3. NMR KINETIC

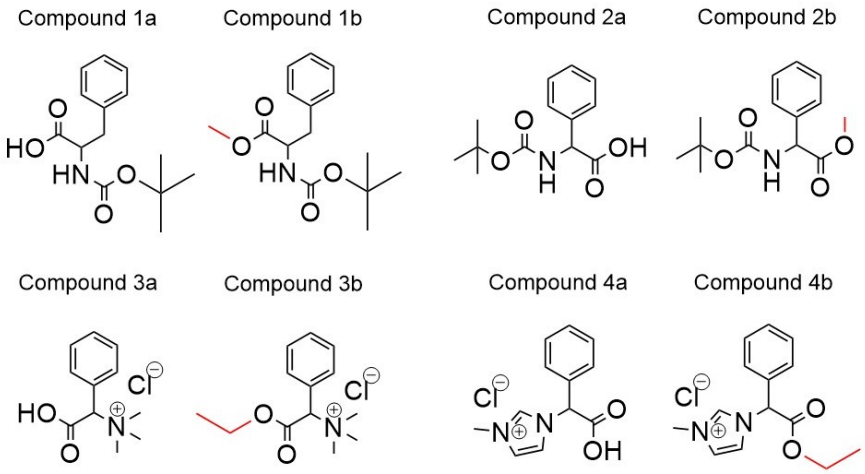

Figure 41. General structures of the compounds that have been used in these studies.

Compound 1

Racemization studies with lithium hydroxide: The NMR tube with pH equal to 8 was prepared by mixing 0.006 mmol of compound 1b (final concentration of 0.01M, stock 0.1 M in deuterated acetonitrile) and 180 μL of LiOH (final concentration of 3×10^{-4} μM, stock in deuterium oxide). The remaining volume was filled in acetonitrile and/or water, thus reaching a final volume of 600 μL and 7:3 proportion of acetonitrile and water respectively. The NMR tube with pH 11 was prepared by placing in solution 0.006 mmol of compound 1a (final concentration of 0.01M, stock 0.1 M in deuterated acetonitrile) and 180 μL of LiOH (final concentration of 3×10^{-1} μM, stock in deuterium oxide). The remaining volume was adjusted with acetonitrile and/or water, reaching the final volume of 600 μL and 7:3 proportion of acetonitrile and water respectively.

Racemization studies with DBU: The NMR tube was realized by placing 1 equivalent of compound 1b (13.97 mg, final concentration of 0.01 M) and 0.5 equivalents of DBU (3.74 μL, final concentration of 0.005 M). The final volume was equal to 600 μL, thus obtaining a final proportion of 7:3 of deuterated DMSO and methanol respectively.

Compound 2

Racemization studies with lithium hydroxide: The tubes were realized following the same procedure seen for compound 1 and using here compound 2b (stock 0.1 M in acetonitrile).

Racemization studies with DBU: 0.006 mmol of compound 2b (final concentration of 0.01 M, stock in deuterated acetonitrile) were placed in solution together with 0.003 mmol of DBU (final concentration of 0.005 M, stock in deuterium oxide). The final volume of 600 μL was reached by adding deuterated acetonitrile and/or water in order to have final solvent proportions equal to 7:3, 8:2, 9:1 and 95:5 of acetonitrile and water respectively. The same procedure was followed for 2a in which NaOD was added to reach the corresponding pH of the ester.

Temperature studies: 0.006 mmol of compound 2b (final concentration of 0.01 M, stock 0.1 M in deuterated acetonitrile) were placed in solution together with 0.003 mmol of DBU (final concentration of 0.005 M, stock 0.1 M in deuterium oxide). The final volume of 600 μL was reached by adding deuterated acetonitrile and/or water in order to have final solvent proportions equal to 7:3, 9:1 of acetonitrile and water respectively. The same procedure was followed for 2a too, using 7:3 proportion.

Compound 3

Racemization studies in water only: 0.006 mmol of 3b (1.81 mg, final concentration of 0.01 M) were placed in solution with 0.120 mmol of buffer (final concentration of 0.2 M, stock 1 M in deuterated water) specific for four different pH values: 7, 8, 9, 11. The final volume (600 μL) was obtained by adding further deuterium oxide to the solution. The tubes were conserved at room temperature.

Racemization studies in acetonitrile and water: 0.006 mmol of 3b (final concentration of 0.01 M, stock 0.1 M in deuterated acetonitrile) were placed in solution with 0.120 mmol of buffer (final concentration of 0.2 M, stock 1 M in deuterium oxide) specific for four different pH values: 7, 8, 9, 11. The final volume (600 μL) was obtained by adding further deuterium oxide and/or deuterated acetonitrile to the solution, thus obtaining 7:3 proportion of inorganic and organic phase respectively. The tubes were conserved at room temperature. The same procedure was followed for the tubes containing 3a.

Temperature studies: 0.006 mmol of 3a (final concentration of 0.01 M, stock 0.1 M in deuterated dimethyl sulfoxide) were placed in solution with 0.120 mmol of buffer borate pH 11 (final concentration of 0.2 M, stock 1 M in deuterium oxide). The final volume (600 μL) was obtained by adding further deuterium oxide and/or deuterated acetonitrile to the solution, thus obtaining 7:3 proportion of inorganic and organic phase respectively. The tube was placed at 50 °C.

Activation studies with MeI: Four experimental conditions were implemented here. The first two tubes were realized by placing in solution 0.006 mmol of 3a (final concentration of 0.01 M, stock 0.1 M in DMSO) together with 0.03 mmol of MeI (final concentration of 0.05 M, stock 0.1 M in CAN). In one of them were added 0.120 mmol of buffer phosphate pH 7 (final concentration of 0.2 M, stock 1M in deuterium oxide). In the other one the pH was maintained at 7 by manual monitoring at the pH meter (DCl or NaOD stock 0.1 M in deuterium oxide). The remaining tubes contained, instead, 0.150 mmol of MeI (final concentration of 0.25 M). The pH equal to 7 was set by 0.2 mmol of phosphate buffer (final concentration of 0.33 M) in one of them, in the other the pH was regulated manually with the pH meter. The final volume equal to 600 μL was reached by adding deterated water and/or acetonitrile to obtain 7:3 proportion between the water and the organic phase.

Activation studies with EDC plus NHS: The first tube contained 0.006 mmol of 3a (final concentration of 0.01 M, stock 0.1 M in DMSO), 0.120 mmol of buffer phosphate (final concentration of 0.2 M, stock 1 M in deuterium oxide), 0.018 mmol of NHS (final concentration of 0.03 M, stock 0.2 M in deuterium oxide), and 0.018 mmol of EDC (final concentration of 0.03 M, stock 0.2 M in DMSO). The final volume of 600 μL was obtained adding deuterated deuterium oxide and DMSO to reach 7:3 proportion of them respectively.

After the first one, the pH of compound 3a stock was adjusted with DCl to obtain a final value of 6, thus the samples will have a final pH of 6. The second tube contained 0.006 mmol of 3a (final concentration of 0.01 M, stock 0.1 M in deuterium oxide), 0.060 mmol of NHS (final concentration of 0.1 M, stock 0.5 M in deuterium oxide), and 0.060 mmol of EDC (11.50 mg, final concentration of 0.1 M). The final volume of 600 µL was obtained adding deuterated deuterium oxide and acetonitrile to reach 7:3 proportion of them respectively.

0.060 mmol of EDC (11.50 mg, final concentration of 0.1 M) was added to 600 µL of deuterium oxide to compose the third tube. After 20 hours, 0.006 mmol of 3a were added to the solution (final concentration of 0.01 M, stock 0.1 M in deuterium oxide). After 3 hours and a half, 0.06 mmol of NHS (final concentration of 0.1 M, stock 0.5 M in deuterium oxide) were added to the previous mixture.

The fourth tube contained 0.006 mmol of 3a (final concentration of 0.01 M, stock 0.1 M in deuterium oxide), 0.060 mmol of NHS (final concentration of 0.1 M, stock 0.5 M in deuterium oxide), and 0.060 mmol of EDC (11.50 mg, final concentration of 0.1 M). The final volume of 600 µL was obtained adding deuterated deuterium oxide and acetonitrile to reach 5:5 proportion.

Activation studies with DIC plus NHS: Two tubes were realized by placing in solution 0.006 mmol of 3a (final concentration of 0.01 M, stock 0.1 M in deuterium oxide, pH adjusted to 5), 0.060 mmol of NHS (final concentration of 0.1 M, stock 0.5 M in deuterium oxide), and 0.060 mmol of DIC (9.28 µL, final concentration of 0.1 M). After the complete transformation of DIC into urea, other 0.060 mmol of NHS and 0.060 mmol of DIC were added. In the tubes deuterated acetonitrile and water were added to reach a final volume of 600 µL and a final proportion between the two phases of 5:5.

Two tubes were realized by placing in solution 0.006 mmol of 3a (final concentration of 0.01 M, stock 0.1 M in deuterium oxide, pH adjusted to 5), 0.060 mmol of NHS (final concentration of 0.1 M, stock 0.5 M in deuterium oxide, pH adjusted to 5), and 0.060 mmol of DIC (9.28 µL, final concentration of 0.1 M). After the complete transformation of DIC into urea, other 0.060 mmol of NHS and 0.060 mmol of DIC were added. Deuterated acetonitrile and water were added to reach a final volume of 600 µL and a final proportion between the two phases of 5:5.

Stability controls of the components: To test DIC stability, 0.060 mmol of DIC (9.28 µL, final concentration of 0.1 M) were added to 600 µL of a solution made by 50% of water and 50% of acetonitrile, both deuterated.

DIC plus NHS. 0.060 mmol of DIC (9.28 µL, final concentration of 0.1 M) and 0.060 mmol of NHS (final concentration of 0.1 M, stock 0.5 M in deuterium oxide, pH adjusted to 5) were added to a solution made by 50% of water and 50% of acetonitrile, both deuterated, with a final volume equal to 600 µL. After the complete transformation of DIC into urea, 0.006 mmol of 3a (final

concentration of 0.01 M, stock 0.1 M in deuterium oxide, pH adjusted to 5) were added to test the stability of 3a in presence of urea.

NHS plus 3a. 0.060 mmol of NHS (final concentration of 0.1 M, stock 0.5 M in deuterium oxide, pH adjusted to 5) and 0.006 mmol of 3a (final concentration of 0.01 M, stock 0.1 M in deuterium oxide, pH adjusted to 5) were added to a 5:5 solution of deuterated acetonitrile and water, with final volume of 600 μL.

DIC plus 3a. 0.060 mmol of DIC (9.28 μL, final concentration of 0.1 M) and 0.006 mmol of 3a (final concentration of 0.01 M, stock 0.1 M in deuterium oxide, pH adjusted to 5) were added to a 5:5 solution of deuterated acetonitrile and water, with final volume of 600 μL.

Compound 4

Racemization studies of 4a: The tube was realized by using 8:2 proportion of water and acetonitrile respectively. 0.006 mmol of 4a (final concentration of 0.01 M, stock 0.076 M in deuterated acetonitrile) and 0.120 mmol of borate buffer (final concentration of 1 M, stock in deuterium oxide, pH 9) were added. Final volume equal to 600 μL.

The tube was realized by using 8:2 proportion of water and acetonitrile respectively. 0.006 mmol of 4a (final concentration of 0.01 M, stock 0.076 M in deuterated acetonitrile) and 0.120 mmol of phosphate buffer (final concentration of 1 M, stock in deuterium oxide, pH 8) were added. Final volume equal to 600 μL.

The tube was realized by using 7:3 proportion of water and acetonitrile respectively. 0.006 mmol of 4a (final concentration of 0.0072 M, stock 0.076 M in deuterated acetonitrile) and 0.120 mmol of borate buffer (final concentration of 1 M, stock in deuterium oxide, pH 11) were added. Final volume equal to 600 μL.

Racemization studies of 4b: The tube was realized by using 5:5 proportion of water and acetonitrile respectively. 0.006 mmol of 4a (final concentration of 0.01 M, stock 0.1 M in deuterated acetonitrile) and 0.120 mmol of phosphate buffer (final concentration of 1 M, stock in deuterium oxide, pH 7) were added. Final volume equal to 600 μL.

5.4. BUFFERS

pH 7: addition of 348.36 mg of potassium phosphate dibasic to 1.5 mL of deuterated water. The pH was measured using a pH meter and adjusted to the desired value by using deuterium chloride. After that, other deuterium oxide was added in order to reach a concentration equal to 0.5 M. The vial containing in the end 4 mL of solution, were placed under azote flux until completely

dried. The final powder was further dissolved in 2 mL of deuterium oxide, obtaining in the end a 1 M solution of the buffer whose pH was tested again and eventually adjusted by adding deuterium chloride or deuterated sodium hydroxide.

pH 8: this buffer was realized as the previous one.

pH 9: addition of 123.66 mg of boric acid to 2.5 mL of deuterium oxide. The pH was measured and adjusted by using a pH meter and by using deuterated sodium hydroxide. After reaching the desired value, the volume was raised to 4 mL and the vial placed under lyophilization until complete desiccation. The resulting powder was then dissolved into 2 mL of deuterium oxide, in order to reach a final concentration equal to 1 M. After that, the pH was further tested and eventually adjusted.

pH 11: this buffer was realized with the same procedure seen for pH 9.

5.5. NMR SPECTRA

Spectrum 1: Kinetic of compound **2b** racemization in 7:3 proportion of deuterated acetonitrile and water.

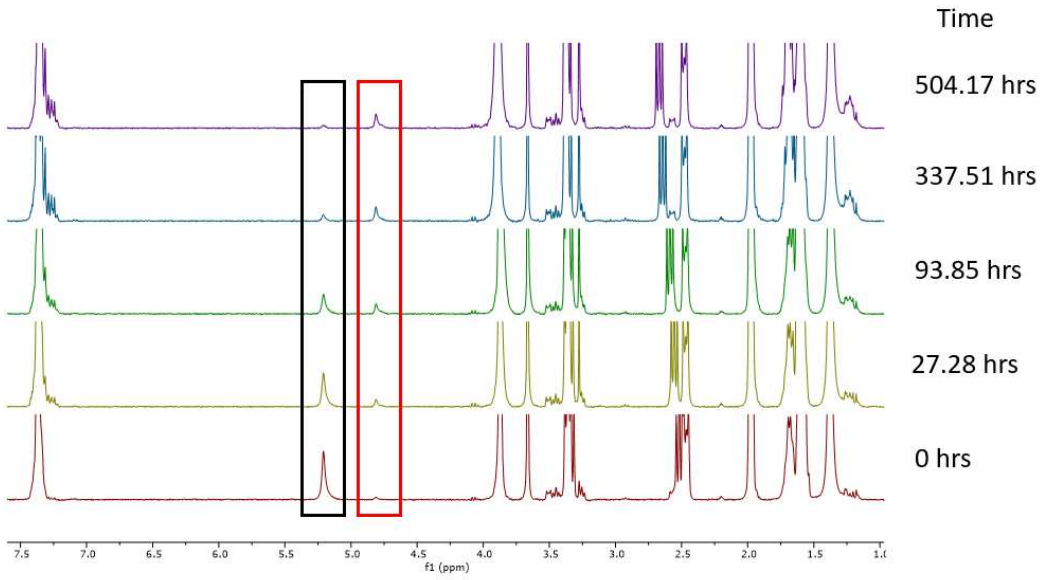

*Figure 42. ^1H spectrum (300 MHz, ACN_{d3} : D_2O 7:3) of kinetic of racemization of compound **2b**. Black rectangle represents the disappearance of ester alpha proton, instead the red one represents the increase in the acid alpha proton.*

Spectrum 2: Kinetic of compound **2b** racemization in 8:2 proportion of deuterated acetonitrile and water.

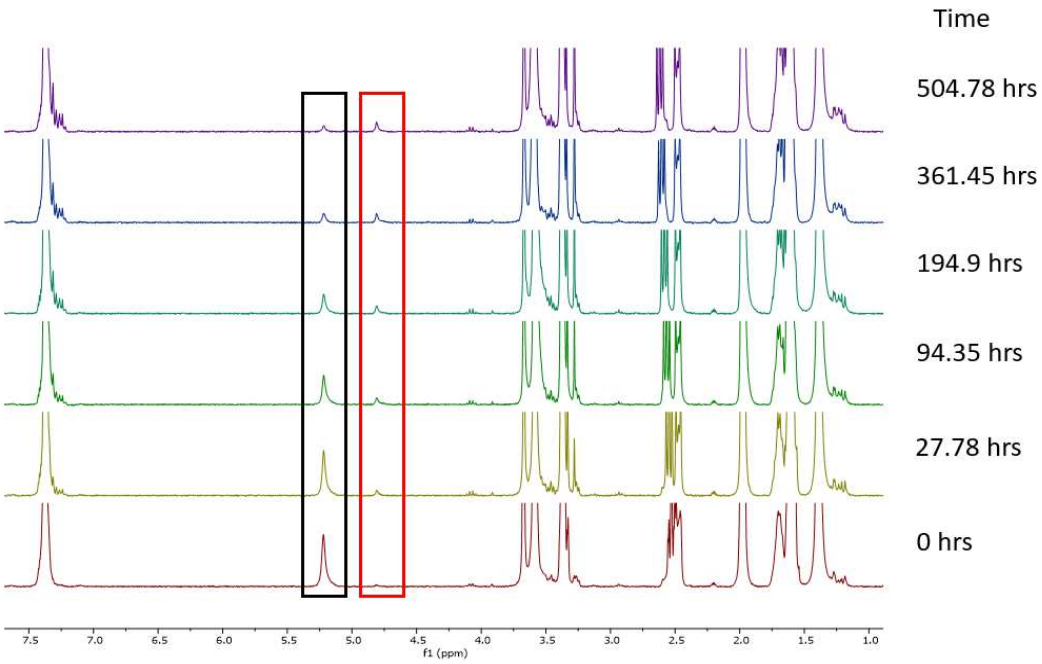

*Figure 43. ^1H spectrum (300 MHz, ACN_{d3} : D_2O 8:2) of kinetic of racemization of compound **2b**. Black rectangle represents the disappearance of ester alpha proton, instead the red one represents the increase in the acid alpha proton.*

Spectrum 3: Kinetic of compound **2b** racemization in 9:1 proportion of deuterated acetonitrile and water.

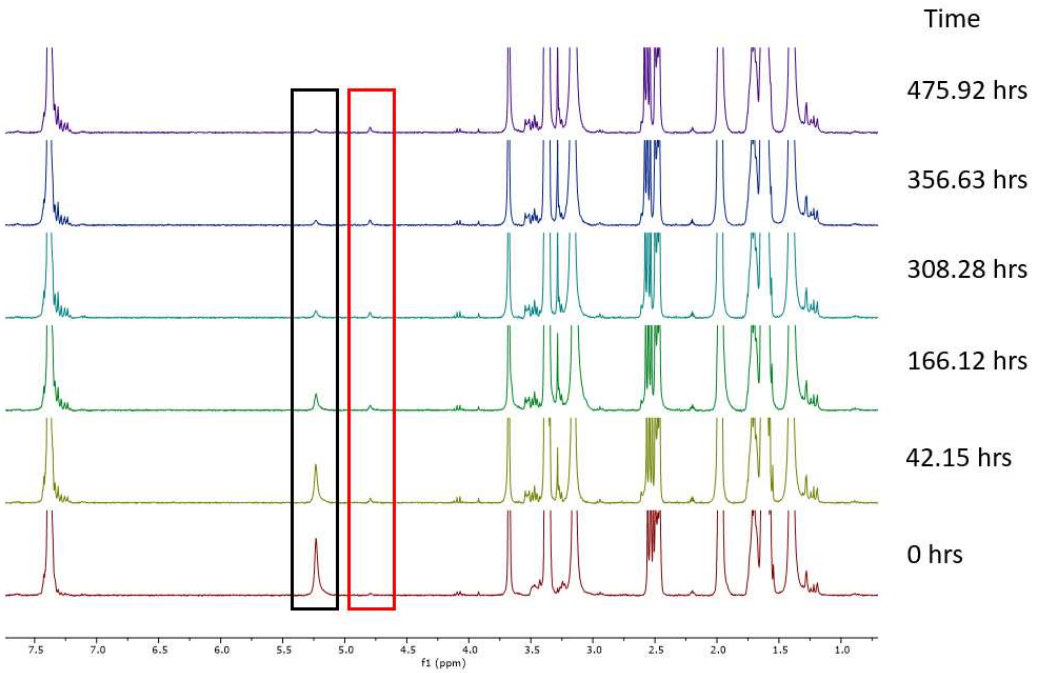

*Figure 44. ^1H spectrum (300 MHz, ACN_{d3} : D_2O 9:1) of kinetic of racemization of compound **2b**. Black rectangle represents the disappearance of ester alpha proton, instead the red one represents the increase in the acid alpha proton.*

Spectrum 4: Kinetic of compound **2b** racemization in 95:5 proportion of deuterated acetonitrile and water.

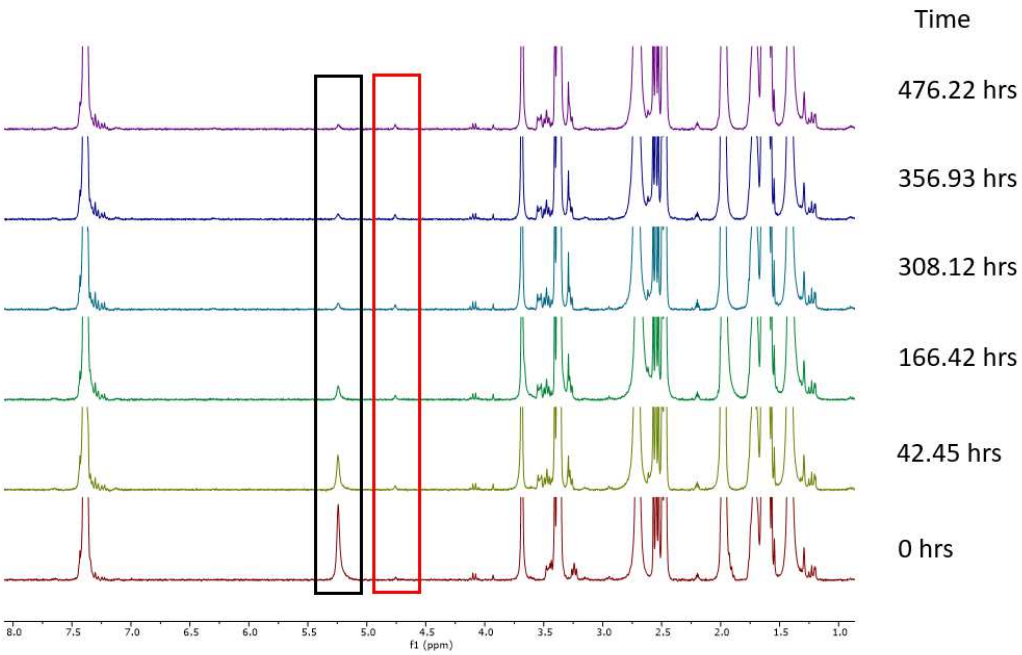

*Figure 45. ^1H spectrum (300 MHz, ACN_{d3} : D_2O 95:5) of kinetic of racemization of compound **2b**. Black rectangle represents the disappearance of ester alpha proton, instead the red one represents the increase in the acid alpha proton.*

Spectrum 5: Kinetic of compound **3b** racemization in 7:3 proportion of deuterated water and acetonitrile, at pH 7.

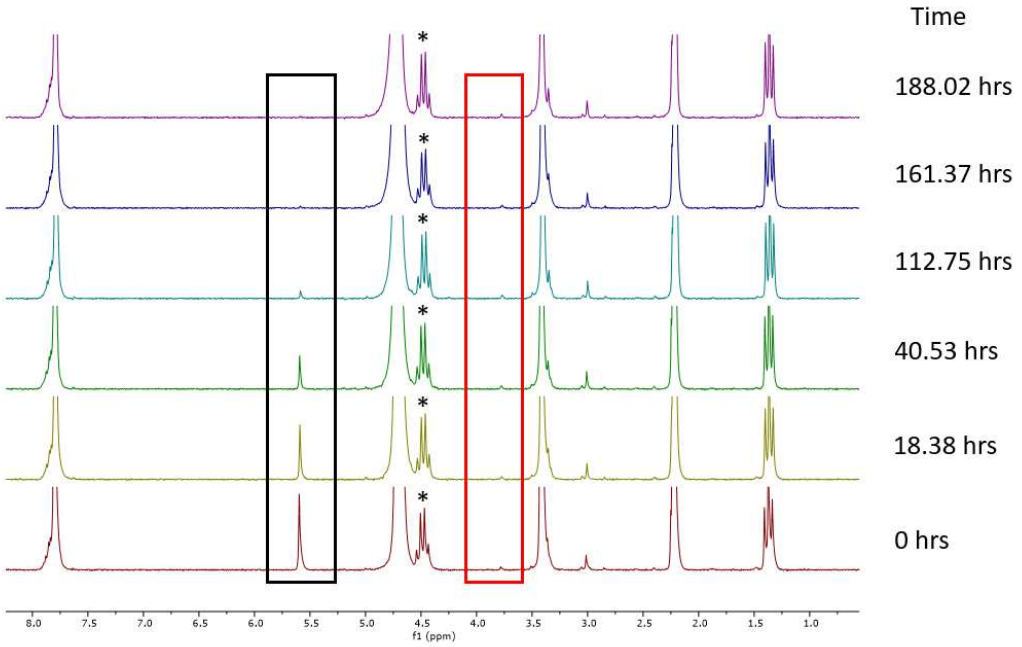

*Figure 46. ^1H spectrum (300 MHz, ACN_{d3} : D_2O 7:3) of kinetic of racemization of compound **3b**. Black rectangle represents the disappearance of alpha proton, instead the red one represents the -CH_2 signal of ethanol. The asterisk indicates the -CH_2 of ethyl group.*

Spectrum 6: Kinetic of compound **3b** racemization in 7:3 proportion of deuterated water and acetonitrile, at pH 8.

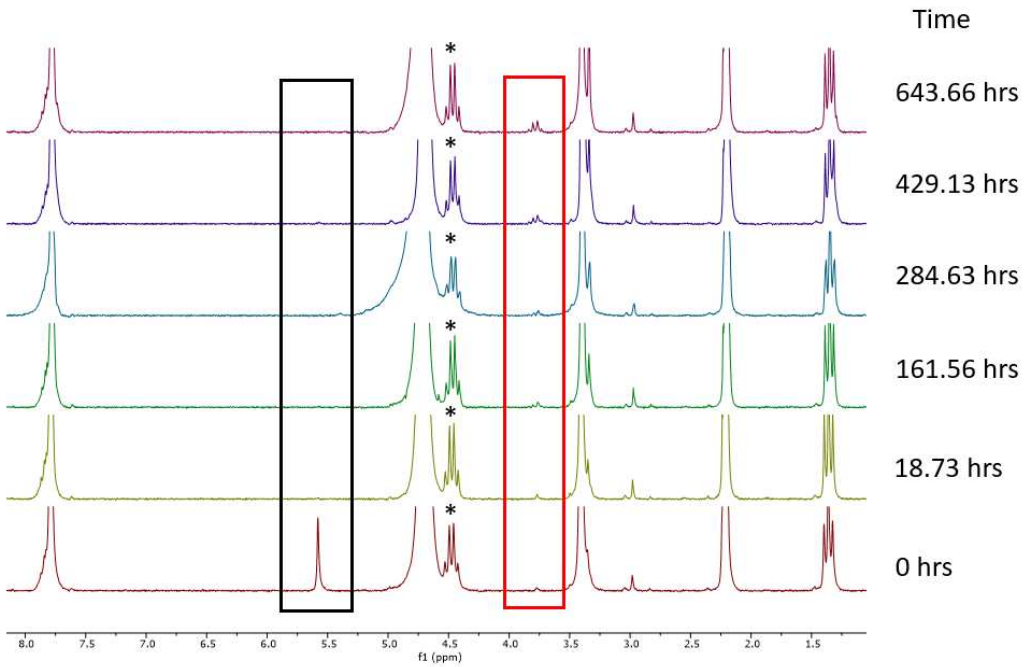

*Figure 47. ^1H spectrum (300 MHz, ACN_{d3} : D_2O 7:3) of kinetic of racemization of compound **3b**. Black rectangle represents the disappearance of alpha proton, instead the red one represents the -CH_2 signal of ethanol. The asterisk indicates the -CH_2 of ethyl group.*

Spectrum 7: Kinetic of compound **3b** racemization in 7:3 proportion of deuterated water and acetonitrile, at pH 9.

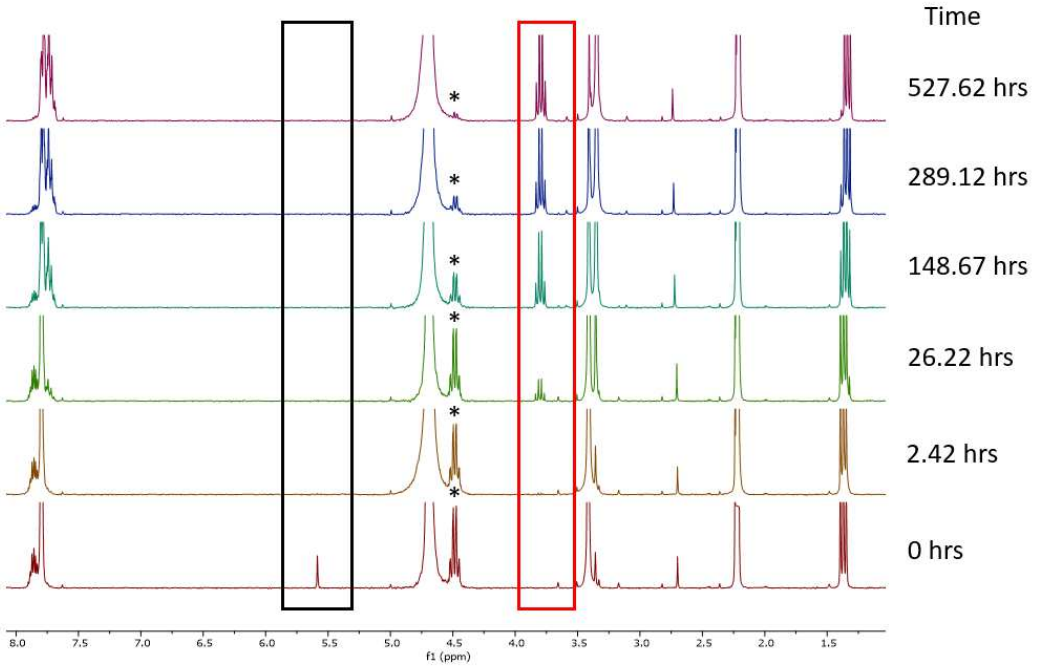

*Figure 48. ^1H spectrum (300 MHz, ACN_{d3} : D_2O 7:3) of kinetic of racemization of compound **3b**. Black rectangle represents the disappearance of alpha proton, instead the red one represents the -CH_2 signal of ethanol. The asterisk indicates the -CH_2 of ethyl group.*

Spectrum 8: Kinetic of compound **3b** racemization in 7:3 proportion of deuterated water and acetonitrile, at pH 11.

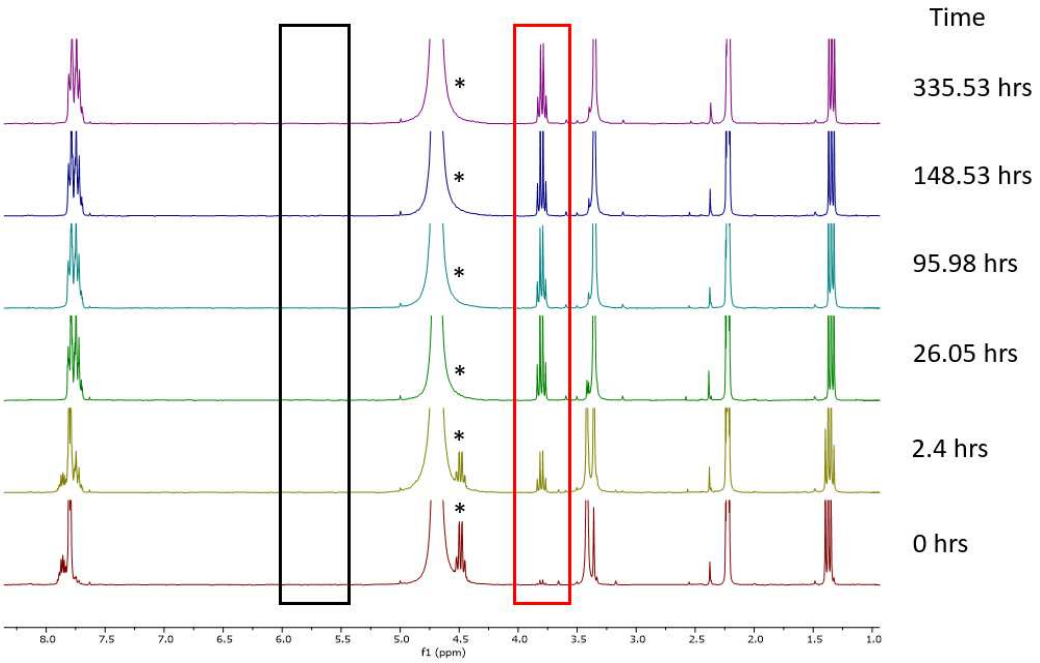

*Figure 49. ^{1}H spectrum (300 MHz, ACN_{d3} : D_2O 7:3) of kinetic of racemization of compound **3b**. Black rectangle represents the disappearance of alpha proton, instead the red one represents the -CH_2 signal of ethanol. The asterisk indicates the -CH_2 of ethyl group.*

Spectrum 9: Kinetic of compound **4a** racemization in 7:3 proportion of deuterated water and acetonitrile, at pH 8.

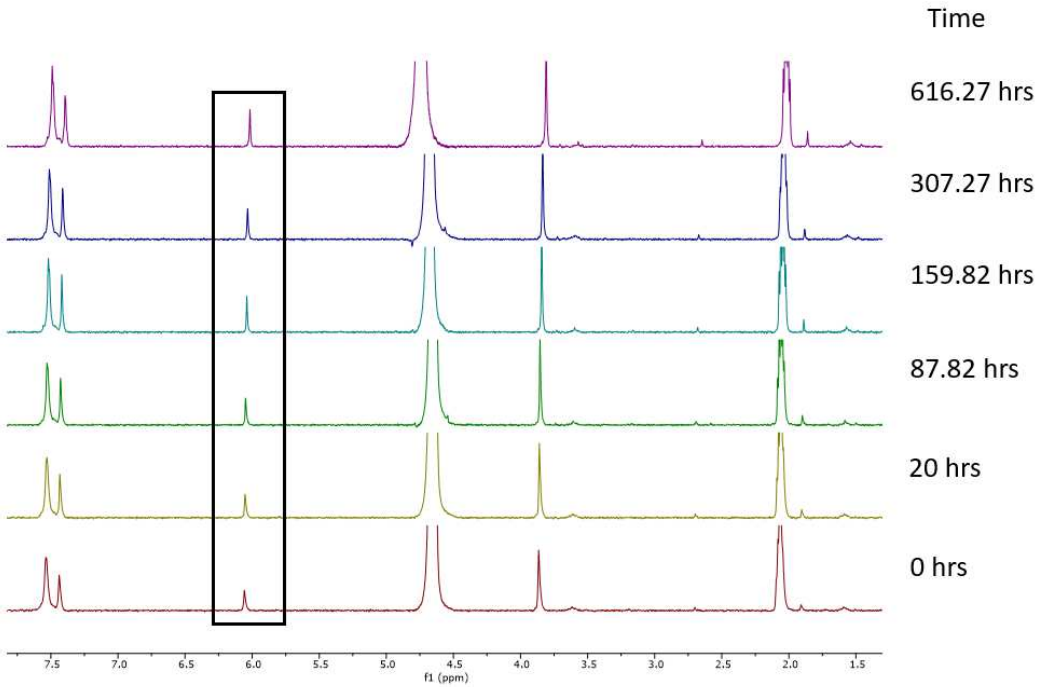

*Figure 50. ^{1}H spectrum (300 MHz, ACN_{d3} : D_2O 7:3) of kinetic of racemization of compound **4a**. Black rectangle represents the disappearance of alpha proton.*

Spectrum 10: Kinetic of compound **4a** racemization in 8:2 proportion of deuterated water and acetonitrile, at pH 9.

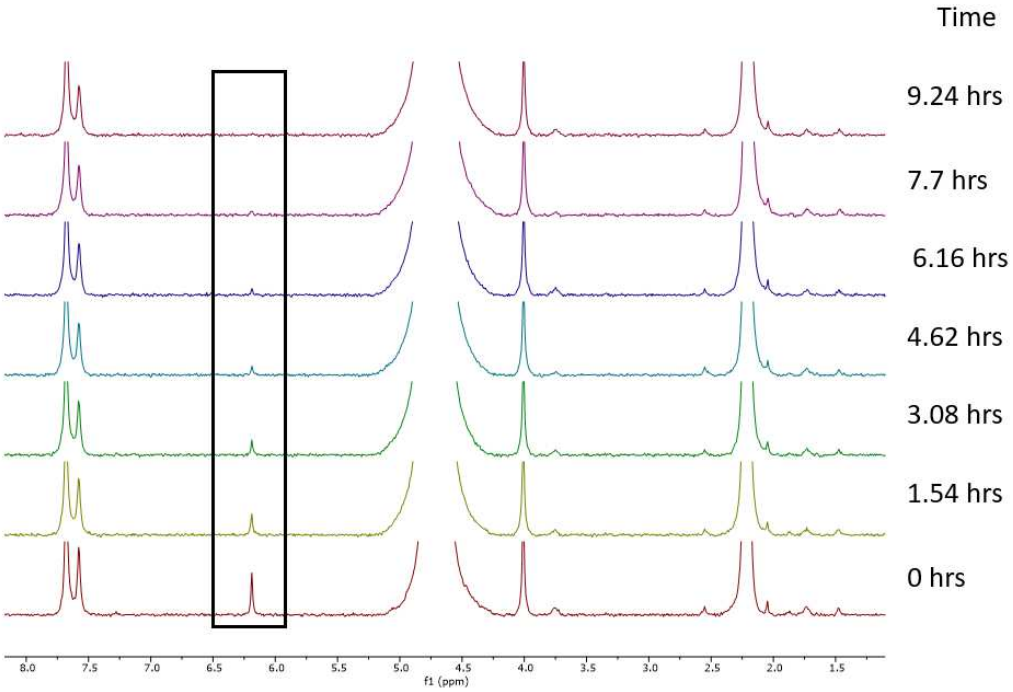

*Figure 51. ^{1}H spectrum (300 MHz, ACN_{d3} : D_2O 8:2) of kinetic of racemization of compound **4a**. Black rectangle represents the disappearance of alpha proton.*

Spectrum 11: Kinetic of compound **4a** racemization in 7:3 proportion of deuterated water and acetonitrile, at pH 11.

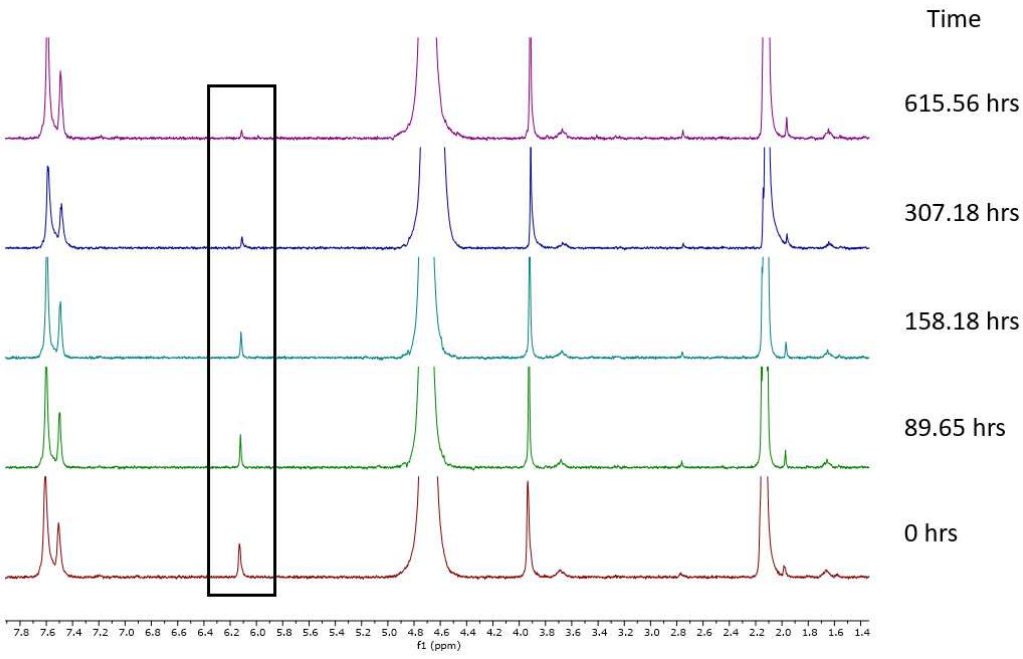

*Figure 52. ^{1}H spectrum (300 MHz, ACN_{d3} : D_2O 8:2) of kinetic of racemization of compound **4a**. Black rectangle represents the disappearance of alpha proton.*

6. REFERENCES

1. E. Schrodinger (1944) "What is life? The physical aspects of living cells." *Cambridge Univ Press, Cambridge, UK*

2. A. P. Davis (1998) "Tilting at Windmills? The Second Law Survives." *Angew. Chem. Int.* 37:909-910

3. S. Borsley, D. A. Leigh, B. M. W. Roberts (2022) "Chemical fuels for molecular machinery." *Nature Chemistry* 14:728-738

4. G. Ragazzon, L. J. Prins (2018) "Energy consumption in chemical fuel-driven self-assembly." *Nature Nanotechnology* 13:882-889

5. K. Das, L. Gabrielli, L. J. Prins (2021) "Chemically-fueled self-assembly in biology and chemistry." *Angew. Chem.Int.* 60:20120–20143

6. J. Boekhoven, A. M. Brizard Dr., K. N. K. Kowlgi, G. J. M. Koper Dr., R. Eelkema Dr., J. H. van Esch Prof. Dr. (2010) "Dissipative Self-Assembly of a Molecular Gelator by Using a Chemical Fuel." *Angew. Chem. 122:4935-4938*

7. J. Boekhoven, W. E. Hendriksen, G. J. M. Koper, R. Eelkema, J. H. van Esch (2015) "Transient assembly of active materials fueled by a chemical reaction." *Science* 349:1075-1079

8. Sisir Debnath, Sangita Roy, and Rein V. Ulijn (2013) "Peptide Nanofibers with Dynamic Instability through Nonequilibrium Biocatalytic Assembly." *J. Am. Chem. Soc.* 135:16789-16792

9. M. Schliwa, G. Woehlke (2003) "Molecular motors." *Nature* 422:759-765

10. S. Borsley, E. Kreidt, D. A. Leigh, B. M. W. Roberts (2022) "Autonomous fuelled directional rotation about a covalent single bond." *Nature* 604:80-85

11. K. Mo, Y. Zhang, Z. Dong, Y. Yang, X. Ma, B. L. Feringa & D. Zhao (2022) "Intrinsically unidirectional chemically fuelled rotary molecular motors." *Nature* 609:293-298

12. Gerson-Gurwitz A, Thiede C, Movshovich N, Fridman V, Podolskaya M, Danieli T, et al. (2011) "Directionality of individual kinesin-5 Cin8 motors is modulated by loop 8, ionic strength and microtubule geometry." *The EMBO journal* 30:4942-4954

13. M. von Delius and D. A. Leigh (2011) “Walking Molecules.” *Chem Soc Rev* 40:3656-3676
14. G. Thejashree, E. Doris, E. Gravel, and I. Namboothiri (2022) “Kinetic and Dynamic Kinetic Resolutions by Dual Catalysis” *Eur. J. Org. Chem.* e202201035

15. B. A. Persson, F. F. Huerta, and J.-E. Backvall (1999) “Dynamic Kinetic Resolution of Secondary Diols via Coupled Ruthenium and Enzyme Catalysis.” *J. Org. Chem.* 64:5237-5240

16. D. A. Schichl, S. Enthaler, W. Holla, T. Riermeier, U. Kragl, and M. Beller (2008) “Dynamic Kinetic Resolution of α-Amino Acid Esters in the Presence of Aldehydes.” *Eur. J. Org. Chem.* 2008:3506-3512

17. S. Amano, M. Esposito, E. Kreidt, D. A. Leigh, E. Penocchio, and B. M. W. Roberts (2022) “Using Catalysis to Drive Chemistry Away from Equilibrium: Relating Kinetic Asymmetry, Power Strokes, and the Curtin−Hammett Principle in Brownian Ratchets.” *J. Am. Chem. Soc.*

18. J. I. Seeman (1986) “The Curtin-Hammett Principle and the Winstein-Holness Equation.” *Journal of Chemical Education* 63:42-48

19. V. Serreli, Chin-Fa Lee, E. R. Kay, D. A. Leigh (2007) “A molecular information ratchet.” *Nature* 445:523-527

20. R. D. Astumian (2019) “Kinetic asymmetry allows macromolecular catalysis to drive an information ratchet.” Nat. Commun. 10:3837

21. L. S. Kariyawasam, M. M. Hossain, C. S. Hartley (2021) “The transient covalent bond in abiotic nonequilibrium systems.” *Angew. Chem. Int. Ed.* 60:12648-12658

22. J. P. Richard, T. L. Amyes, M. M. Toteva (2001) “Formation and stability of carbocations and carbanions in water and intrinsic barriers to their reactions.” *Acc. Chem. Res.* 34:981-988

23. P. D’Arrigo, D. Arosio, L. Cerioli, D. Moscatelli, S. Servi, F. Viani, D. Tessaro (2011) “Base catalyzed racemization of amino acids derivatives.” *Tetrahedron: Asymmetry* 22:851-856

24. J. Crugeiras, A. Rios, E. Riveiros, T. L. Amyes, and John P. Richard (2008) “Glycine Enolates: The Effect of Formation of Iminium Ions to Simple Ketones on r-Amino Carbon Acidity and a Comparison with Pyridoxal Iminium Ions.” *J. Am. Chem. Soc.* 130:2041-2050

25. D. Arosio, A. Caligiuri, P. D'Arrigo, G. Pedrocchi-Fantoni, C. Rossi, C. Saraceno, S. Servi and D. Tessaroa (2007) "Chemo-Enzymatic Dynamic Kinetic Resolution of Amino Acid Thioesters." *Adv. Synth. Catal* 349:1345-1348

26. A. Williams, and I. T. Ibrahim (1981) "Carbodiimide Chemistry: Recent Advances." Chem. Rev. 81:589-636

27. J. Crugeiras, A. Rios, E. Riveiros, and J. P. Richard (2011) "Substituent Effects on Electrophilic Catalysis by the Carbonyl Group: Anatomy of the Rate Acceleration for PLP-Catalyzed Deprotonation of Glycine." *J. Am. Chem. Soc.* 133:3137-3183

28. P. J. Hore "Nuclear magnetic resonance." 3rd edition, Oxford University Press, 2015

29. S. K. Vashist (2012) "Comparison of 1-Ethyl-3-(3-Dimethylaminopropyl) Carbodiimide Based Strategies to Crosslink Antibodies on Amine-Functionalized Platforms for Immunodiagnostic Applications." *Diagnostics* 2:23-33

30. Thermo Scientific Instructions "NHS and Sulfo-NHS."

31. Z. Grabarek, and J. Gergely (1990) "Zero-length crosslinking procedure with the use of active esters." *Anal Biochem* 185:131-5.

32. K. Basu, A. Baral, S. Basak, A. Dehsorkhi, J. Nanda, D. Bhunia, S. Ghosh, V. Castelletto, I. W. Hamleyb and A. Banerjee (2016) "Peptide based hydrogels for cancer drug release: modulation of stiffness, drug release and proteolytic stability of hydrogels by incorporating d-amino acid residue(s)." Chem. Comm. 52 (28):5045-5048

33. P. Fatás, J. Bachl, S. Oehm, A. I Jiménez, C. Cativiela, D. D. Díaz (2013) "Multistimuli-responsive supramolecular organogels formed by low-molecular-weight peptides bearing side-chain azobenzene moieties." *Chemistry* 19:8861-8874

34. A. Belardini, E. Petronijevic, R. Ghahri, D. Rocco, F. Pandolfi, C. Sibilia and L. Mattiello (2021) "Fluorescence Spectroscopy of Enantiomeric Amide Compounds Enforced by Chiral Light." *Appl. Sci.* 11:11375